QEX

July/August 2021

www.arrl.org

A Forum for Communications Experimenters

Issue No. 327

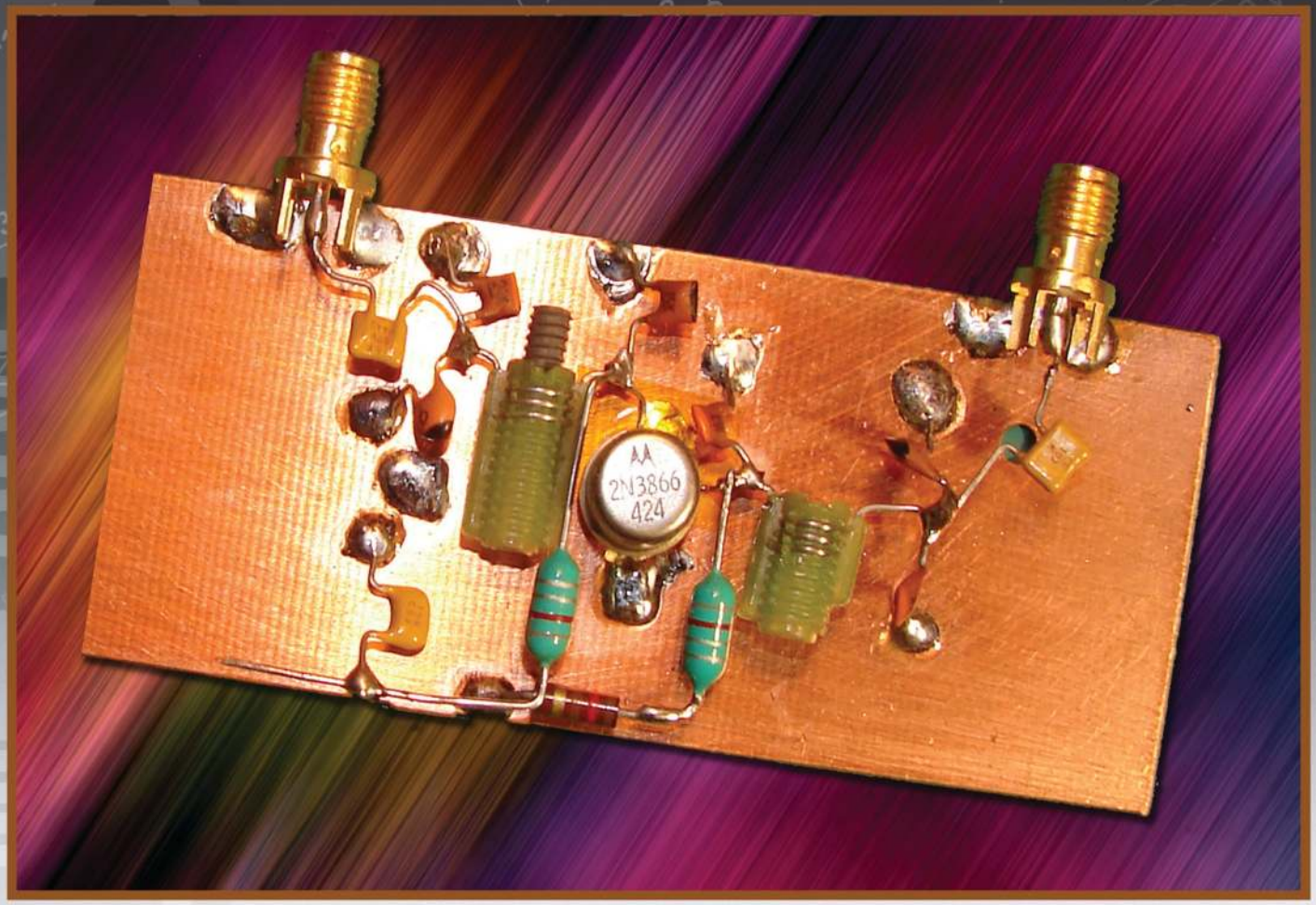

W4AMV presents a technique for designing Class C power amplifiers.

The EVENT HORIZON OF DX

TS-990S

Dual TFT Display & Dual Receiver HF/50 MHz Transceiver

The main receiver has an IP3 in the +40 dB class, and the sub receiver is the already famous TS-590S receiver. Capable of receiving two signals at once, on different bands. 7-inch and 3.5-inch color TFT displays allow displaying of independent contents. Simplification of complex operations at a glance. Make no mistake, this is not a toy. Finally a serious tool is available for getting the very most from your hobby, of course it's a Kenwood.

- Covers the HF and 50 MHz bands.
- High-speed automatic antenna tuner.
- USB, Serial and LAN ports.
- Various PC applications (free software): ARCP-990 enabling PC control, ARHP-990 enabling remote control, and ARUA-10 USB audio driver.
- Clean 5 to 200 W transmit power through the 50 V FET final unit.
- Built-in RTTY and PSK.
- Three Analog Devices 32-bit floating-point arithmetic DSPs.
- DVI output for display by an external monitor (main screen display only).

KENWOOD

Customer Support: (310) 639-4200
Fax: (310) 537-8235

www.kenwood.com/usa

ISO9001 Registered

ADS#05421

QEX

QEX (ISSN: 0886-8093) is published bimonthly in January, March, May, July, September, and November by the American Radio Relay League, 225 Main St., Newington, CT 06111-1400. Periodicals postage paid at Hartford, CT and at additional mailing offices.

POSTMASTER: Send address changes to: QEX, 225 Main St., Newington, CT 06111-1400
Issue No. 327

Publisher
American Radio Relay League

Kazimierz "Kai" Siwiak, KE4PT
Editor

Lori Weinberg, KB1EIB
Assistant Editor

Scotty Cowling, WA2DFI
Ray Mack, W5IFS
Contributing Editors

Production Department

Becky R. Schoenfeld, W1BXY
Publications Manager

Michelle Bloom, WB1ENT
Production Supervisor

David Pingree, N1NAS
Senior Technical Illustrator

Brian Washing
Technical Illustrator

Advertising Information

Janet L. Rocco, W1JLR
Business Services
860-594-0203 – Direct
800-243-7768 – ARRL
860-594-4285 – Fax

Circulation Department

Cathy Stepina
QEX Circulation

Offices

225 Main St., Newington, CT 06111-1400 USA
Telephone: 860-594-0200
Fax: 860-594-0259 (24-hour direct line)
Email: **qex@arrl.org**

Subscription rate for 6 print issues:

In the US: $29

US by First Class Mail: $40;

International and Canada by Airmail: $35

ARRL members receive the digital edition of *QEX* as a member benefit.

In order to ensure prompt delivery, we ask that you periodically check the address information on your mailing label. If you find any inaccuracies, please contact the Circulation Department immediately. Thank you for your assistance.

About the Cover

Alan Victor, W4AMV, applies and verifies *Spice* models and FFT techniques to a systematic design flow for Class C RF power amplifiers in the 1-to-10 watt class that are used as bipolar drivers or final amplifiers in a small transmitter. The approach includes finding the required impedance transforming circuits, power gain and efficiency. All of this capability is provided by freely available software and simple tools that are easy to implement and support in a modest lab environment. The outlined approach can also be applied to Class C designs for MOSFETS, IGFETs and larger bipolar devices.

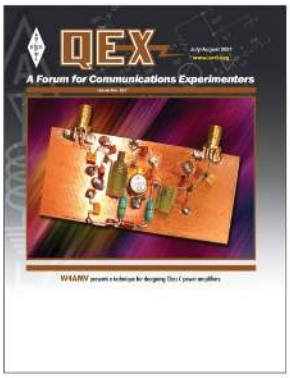

In This Issue

Index of Advertisers

The American Radio Relay League

The American Radio Relay League, Inc., is a noncommercial association of radio amateurs, organized for the promotion of interest in Amateur Radio communication and experimentation, for the establishment of networks to provide communications in the event of disasters or other emergencies, for the advancement of the radio art and of the public welfare, for the representation of the radio amateur in legislative matters, and for the maintenance of fraternalism and a high standard of conduct.

ARRL is an incorporated association without capital stock chartered under the laws of the state of Connecticut, and is an exempt organization under Section 501(c)(3) of the Internal Revenue Code of 1986. Its affairs are governed by a Board of Directors, whose voting members are elected every three years by the general membership. The officers are elected or appointed by the Directors. The League is noncommercial, and no one who could gain financially from the shaping of its affairs is eligible for membership on its Board.

"Of, by, and for the radio amateur," ARRL numbers within its ranks the vast majority of active amateurs in the nation and has a proud history of achievement as the standard-bearer in amateur affairs.

A *bona fide* interest in Amateur Radio is the only essential qualification of membership; an Amateur Radio license is not a prerequisite, although full voting membership is granted only to licensed amateurs in the US.

Membership inquiries and general correspondence should be addressed to the administrative headquarters:

ARRL
225 Main St.
Newington, CT 06111 USA
Telephone: 860-594-0200
FAX: 860-594-0259 (24-hour direct line)

Officers

President: Rick Roderick, K5UR
P.O. Box 1463, Little Rock, AR 72203

The purpose of *QEX* is to:

1) provide a medium for the exchange of ideas and information among Amateur Radio experimenters,

2) document advanced technical work in the Amateur Radio field, and

3) support efforts to advance the state of the Amateur Radio art.

All correspondence concerning *QEX* should be addressed to the American Radio Relay League, 225 Main St., Newington, CT 06111 USA. Envelopes containing manuscripts and letters for publication in *QEX* should be marked Editor, *QEX*.

Both theoretical and practical technical articles are welcomed. Manuscripts should be submitted in word-processor format, if possible. We can redraw any figures as long as their content is clear. Photos should be glossy, color or black-and-white prints of at least the size they are to appear in *QEX* or high-resolution digital images (300 dots per inch or higher at the printed size). Further information for authors can be found on the Web at **www.arrl.org/qex/** or by e-mail to **qex@arrl.org**.

Any opinions expressed in *QEX* are those of the authors, not necessarily those of the Editor or the League. While we strive to ensure all material is technically correct, authors are expected to defend their own assertions. Products mentioned are included for your information only; no endorsement is implied. Readers are cautioned to verify the availability of products before sending money to vendors.

Kazimierz "Kai" Siwiak, KE4PT

Perspectives

New Rules on RF Exposure Compliance

A lengthy 2019 *RF Report and Order* that went into effect on May 3, 2021 details rule changes governing RF exposure standards. The new rules do not change existing RF exposure limits but do require that stations, including amateur radio stations, be evaluated against existing limits, unless they are exempted. The 2019 *Report and Order* changes the methods that parties use to determine and achieve compliance with FCC limits on human exposure to RF electromagnetic fields.

One of the consequences is that the new rules no longer necessarily exempt handheld transceivers used by hams from certification that their use will comply with a specific absorption rate (SAR) limit. This is new to the amateur radio community, but has historically always been a requirement for commercial handheld transceivers — those used outside the amateur radio service.

The ARRL RF Safety Committee, chaired by Dr. Gregory Lapin, N9GL, is monitoring the new regulatory requirements and working to develop appropriate methods to help hams in their compliance efforts. Simultaneously, a small group of UK amateurs in the Radio Society of Great Britain (RSGB) along with the ARRL in the US have been convening since mid-2020 to collaboratively attack the issues regarding proposed new RF rules to be administered by Ofcom in the UK, and how the new changes in the FCC rules are being applied to hams in the US. Stay tuned!

In This Issue

- Ric Tell, K5UJU, recounts how new FCC rules might now require RF exposure compliance using specific absorption rate (SAR) limits.
- Alan Victor, W4AMV, applies a systematic design flow for Class C RF power amplifiers.
- Tony Brock-Fisher, K1KP, describes a fixture for measuring Q of inductors.
- Jacek Pawlowski, SP3L, investigates the design of antennas considering common mode currents on the transmission line.
- Dan Koellen, AI6XG, uses *Telegram* to remotely command and monitor his ham station.
- John Stanley, K4ERO, matches twinlead or ladder line feeders with a sleeve implementation of a series-section transformer.

Writing for *QEX*

Please keep the full-length *QEX* articles flowing in, or share a **Technical Note** of several hundred words in length plus a figure or two. *QEX* is edited by Kazimierz "Kai" Siwiak, KE4PT, (**ksiwiak@arrl.org**) and is published bimonthly. *QEX* is a forum for the free exchange of ideas among communications experimenters. All members can access digital editions of all four ARRL magazines: *QST*, *On the Air, QEX*, and *NCJ* as a member benefit. The *QEX printed edition* is available at an annual subscription rate (6 issues per year) for members and non-members, see **www.arrl.org/qex**.

Would you like to write for *QEX*? We pay $50 per published page for full articles and *QEX* Technical Notes. Get more information and an Author Guide at **www.arrl.org/qex-author-guide**. If you prefer postal mail, send a business-size self-addressed, stamped (US postage) envelope to: *QEX* Author Guide, c/o Maty Weinberg, ARRL, 225 Main St., Newington, CT 06111.

Very kindest regards,
Kazimierz "Kai" Siwiak, KE4PT
QEX Editor

Alan Victor, W4AMV

8809 Ross Ct., Raleigh, NC 27613; **avictor73@hotmail.com**

A Systematic Design Approach to RF Power Amplifiers

Application and verification of current Spice models and FFT lead to a design flow for Class C RF power amplifiers.

There are a number of circuits that are considered staples to the radio communications enthusiasts. They include oscillators, mixers, power supplies, amplifiers, filters and matching networks. These are but a few, however each should have a cohesive approach to their design and implementation if at all possible. Within each of these classes of circuits there exist sub classes that represent special applications and requirements when integrated with other circuits. The amplifier is representative of this property as there are low noise, linear, wideband, high power and high efficiency designs that are unique in their own approach to design. Many of these circuits might follow a variety of design paths. However, it would be beneficial if at least one unified path might be identified to treat their design.

This article focuses on the Class C RF power amplifier, which finds applications in the 1-to-10 watt class as a low power driver or final amplifier in a small transmitter. After looking at a variety of texts, published literature and handbooks, it was clear that two avenues of design existed. One, either highly simplistic and not able to deliver the required design routine or two, overly complicated and circuit specific. Furthermore, these complex design approaches although delivering extraordinary results are not easy to implement or support within the scope of a modest lab environment.

In this article I discuss a straightforward technique for approaching the design of non-linear RF power amplifiers operating Class C. This includes finding the required impedance transforming circuits, power gain and efficiency. All of this capability is provided by freely available software and simple tools!

Overview

The RF power amplifier design flow presented here makes use of device models if provided. Many excellent *Spice* models exist for the bipolar and FET devices. RF devices must provide characterization data particularly for power amplifier as the device is operated in a nonlinear regime. *Spice* simulation tools **[1]**, **[2]** are freely available and several incorporate device models within the tool. Scattering parameters are another tool, and computer aided tools which process these parameters are presented. Scattering parameter equations provided in this paper are presented without proof. However, Gonzalez **[3]** provides an excellent resource and detail on the equation derivations. As a precursor to device models, Scattering (S) parameters serve a dual role. One, they assist in validation of the model and two, they provide a reasonable first pass design to the power amplifier if models are not available.

Central to the amplifier design is selection of a load impedance that either maximizes the output power or the efficiency. The efficiency is either the dc conversion efficiency, the ratio of RF output power to dc input power, $(P_{out} / P_{dc}) \times 100\%$, or the power added efficiency, *PAE*. The power added efficiency factors in the gain of the amplifier and is a measure of how much of the input signal power is responsible for providing the output power. The *PAE* is defined as,

$$PAE = \frac{(P_{\text{out}} - P_{\text{in}})}{P_{\text{dc}}} \times 100\%.$$

While a high dc conversion efficiency is important, its impact is severely limited if the power gain is small. If *PAE* is rewritten in terms of the dc conversion efficiency and the power gain, the impact of power gain, G_p on efficiency becomes clearer if the gain is below 10 dB. As power gain decreases, so does the efficiency.

$$PAE = DC_{\text{eff}} \times \left(1 - \frac{1}{G_{\text{p}}}\right).$$

Assistance in maximizing the *PAE* is possible by calling on the S-parameters of the device to guide the design of the amplifier. However, because the S-parameters are obtained with small signal device input, they are not totally applicable in the final determination of the amplifier component values. Larger signal excitation is required and for this work calling on the *Spice* model is required. This model with the application of the Fourier series permits the distortion that results to be used in design of the supporting circuits for the power amplifier. It is interesting to note that some similarity to vacuum tube power amplifier designs crossover to semiconductor devices. Conduction angle tagged to efficiency and output power tagged to load impedance are two.

Test Bed and Design Procedure

The test bed consists of a typical 1 to 2 W bipolar device for which S-parameters and *Spice* models are available. The MRF3866 as well the 2N3866 are used to help validate the design procedure. Additionally, newly released RF devices are now characterized with so called large signal parameters. These parameters can be obtained from the *Spice* models if they are not already provided by the device manufacturer. However, the S-parameters are an important guide to the approximate location of the larger signal impedance parameters. This is discussed in the **Model Validation** section.

The test bed application is operated at 200 MHz, high enough in frequency compared to HF to uncover another serious problem in amplifier construction and design: parasitic elements. **Figure 1** illustrates the test bed while **Figure 2A** points to the simulation model that supports the design procedure. The model parameters, **Figure 2B**, include required definitions for the bipolar device and package **[4]**.

Supporting circuits and part of the model simulation must include bias tees or bias feed and input and output impedance transformers. The device model must include the device itself including an accurate package model, for example, a TO-39 or TO-220. In the case of the MRF3866, I needed to convert the model to the proper package for a 2N3866, a T0-39. I first drew a *Spice* model by stripping out the surface mount package, SO8, and then reinserted the device back into a TO-39 package model **[5]**.

Model Validation

Before starting a design, the *Spice* model must be validated. Small signal S-parameters are ideal. Older devices for which many *Spice* models do exist are validated by using other parameter sets such as the hybrid or H parameters or Y, the admittance parameters. These are easily converted to S parameters **[6]**. The MRF3866 model is available and is the SO-8 packaged version of the 2N3866 TO-39 package, popular to QRP enthusiasts. The device model is wrapped in a package model, which depicts the bond wire inductance and capacitance coupling between the bond wires and the lead frame of the package outline. The package and device model are shown in **Figure 3**.

Validation of the model requires setting the model into a bias circuit and adjusting the supply voltage and collector current the same as the measured data **[7]**. Not unlike an actual test bench, the device is connected to a set of bias tees, which provide the base and collector voltage in a setting that does not affect the device measurement. In other words, the bias networks are totally transparent. The test set is shown in **Figure 4**.

The *LTspice* simulator **[8]** provides S-parameter analysis by applying a simple one-line directive into the *Spice* list: .net I(RL) V1 as shown in **Figure 4**. Note, the V1 is the source V but it can take on any convenient number designation. The S-parameters supplied by manufacturers are usually based in a 50 Ω characteristic impedance, hence the voltage generator V1 series R, RS and the load, RL, are set to 50 Ω. The measurement is a small signal measurement. The analysis is simply an

Figure 1 — The small RF power amplifier test set using a 2N3866, center with attached heat sink. RF input is on the left, and output is on the right.

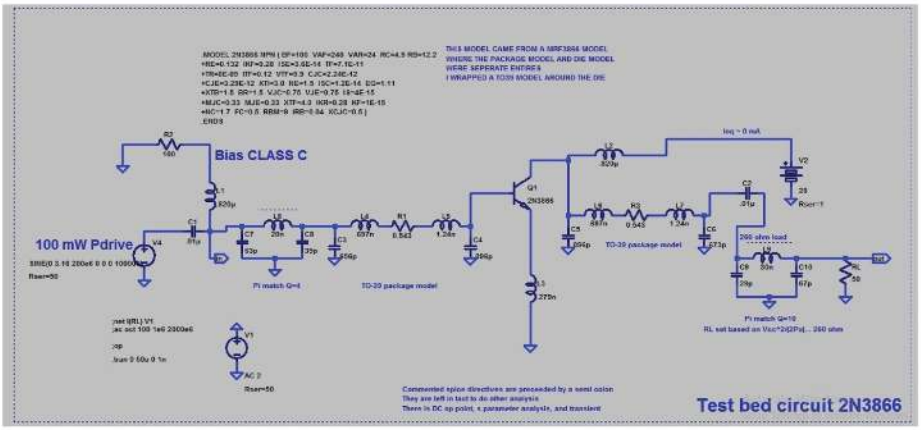

(A)

```
.MODEL 2N3866 NPN ( BF=100  VAF=240  VAR=24  RC=4.9 RB=12.2
+RE=0.132  IKF=0.28  ISE=3.6E-14  TF=7.1E-11
+TR=8E-09  ITF=0.12  VTF=9.9  CJC=2.24E-12
+CJE=3.29E-12  XTI=3.0  NE=1.5  ISC=1.2E-14  EG=1.11
+XTB=1.5  BR=1.5  VJC=0.75  VJE=0.75  IS=4E-15
+MJC=0.33  MJE=0.33  XTF=4.0  IKR=0.28  KF=1E-15
+NC=1.7  FC=0.5  RBM=9  IRB=0.04  XCJC=0.5 )
.ENDS
```

(B)

Figure 2A — Test bed model in Spice including the amplifier impedance transforming circuits. The MRF3866 model is used for the 2N3866 while the package model is modified from SO-8 to TO-39. Figure 2B — Spice model parameters for MRF3866 device or die. These same parameters are used for the 2N3866 model.

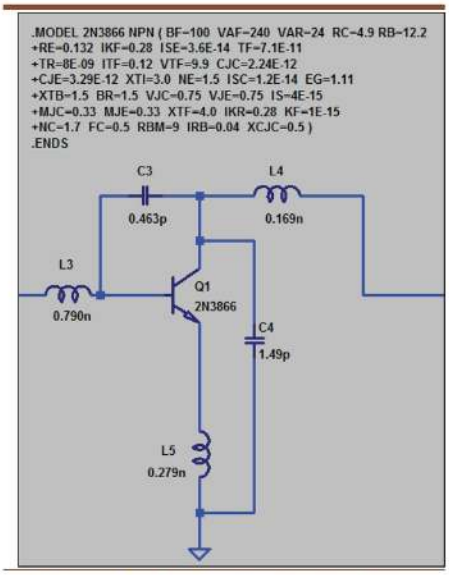

Figure 3 — The 2N3866 device die is wrapped in a SO-8 package model. The resulting device is the MRF3866. Just the device model is extracted and subsequently placed into a TO-39 package model.

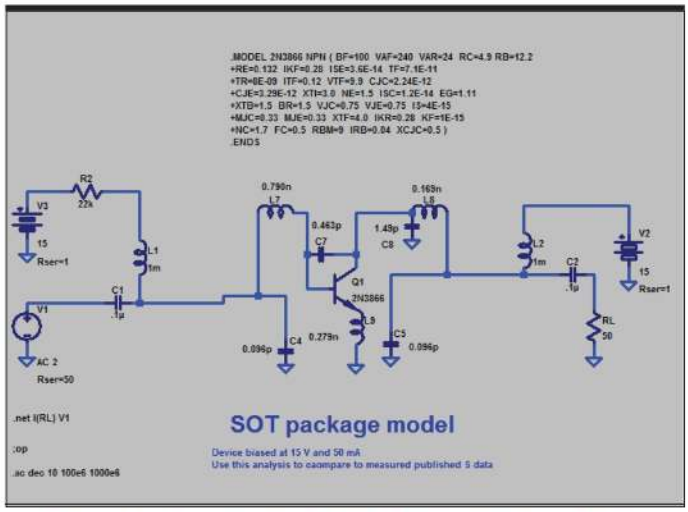

Figure 4 — S-parameter validation test set in Spice for the MRF3866 die in a SO package.

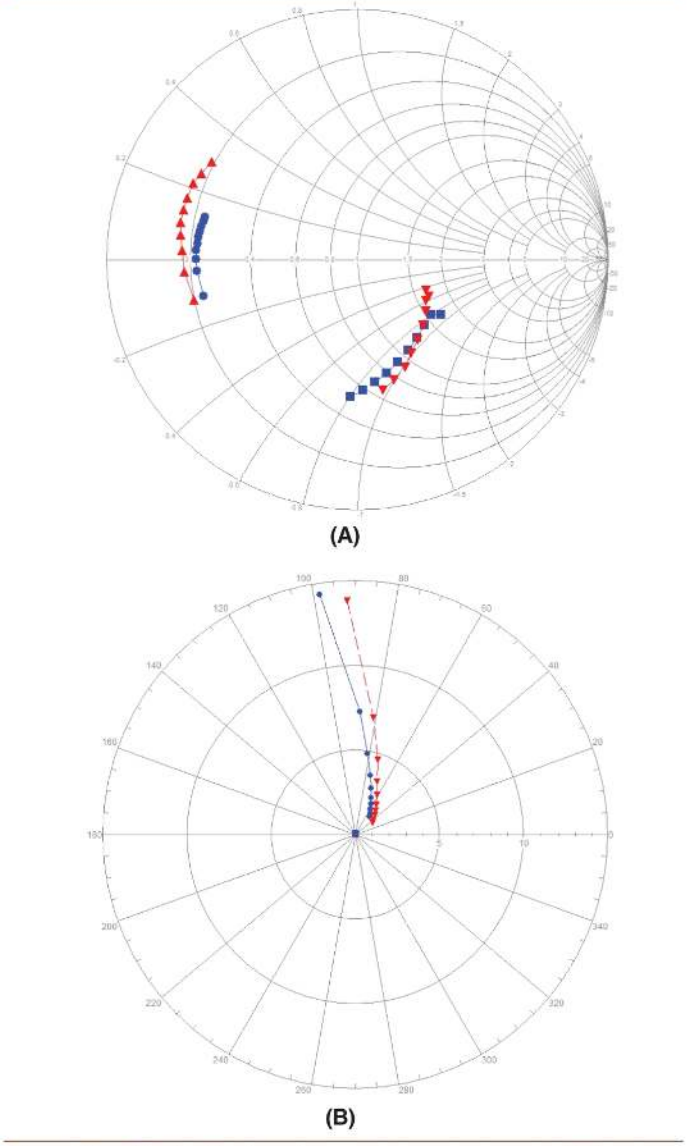

Figure 5A — Model (circle and square) versus measured (triangles), S11 and S22, Smith chart. Figure 5B — The S21 polar chart model (circle), measured (triangle) all vs. frequency 100 MHz to 1 GHz with dc power at 15 V and 50 mA of collector current.

ac analysis. No transient or large input signal voltage is applied to the input of the device. The S-parameter results provided by *Spice* may be analyzed within the *LTspice* framework using its feature of waveform arithmetic. Or, the results are exported to a text file and then inputted to another freeware program, *AppCAD* **[9]**. A feature of this utility is the ability to compare multiple S-parameter files and the inclusion of a detailed Smith chart. Hence, I can easily compare model to simulation, as shown in **Figure 5A** and **Figure 5B**; this is an important step in model validation.

Key to moving forward with a RF power amplifier design is to ensure amplifier stability. As part of model validation, calculation of the stability factor or K is useful.

$$K = \frac{\left|S_{11}S_{22} - S_{12}S_{21}\right|^2 + 1 - \left|S_{11}\right|^2 - \left|S_{22}\right|^2}{2\left|S_{12}\right|\left|S_{21}\right|}.$$

Since the K factor includes all four of the S-parameters, both magnitude and phase, calculation of K is useful for uncovering any model disparity. **Figure 6** shows the case for this model, the MRF3866.

It is important to note that $K > 1$ is a necessary condition to ensure device stability. Hence, this device requires no added circuits to assist in that goal. However, note as the frequency decreases the trend line for K appears to fall below unity. Below 100 MHz, if care is not exercised in the design of the RF power amplifier, instability may occur. This instability can appear as self-oscillation or unusual behavior in the signal output power with increased input power. A proper model will duplicate these highly nonlinear responses while running a transient response simulation in *Spice*.

It is worthy noting that the S-parameters are a reasonable guide to the approximate location of the large signal impedance parameters mentioned earlier. These large signal Z parameters exist for various other classes of amplifier operation. This includes $AB_{1,2}$ where the 1,2 subscript distinguish the variation in amplifier current conduction angle between 180° and 360°, Class B at 180° and Class C, less than 180°.

If the device is inherently stable or can be modified by feedback to achieve stability, then a search region exists for finding the source and load terminations for reasonable amplifier performance. This performance objective goes beyond power and efficiency and can include linearity and reduction in intermodulation distortion. Commercial test beds utilize a technique known as load pull or source pull, so called termination pulls. This operation facilitates a range of device termination impedances and can assess the

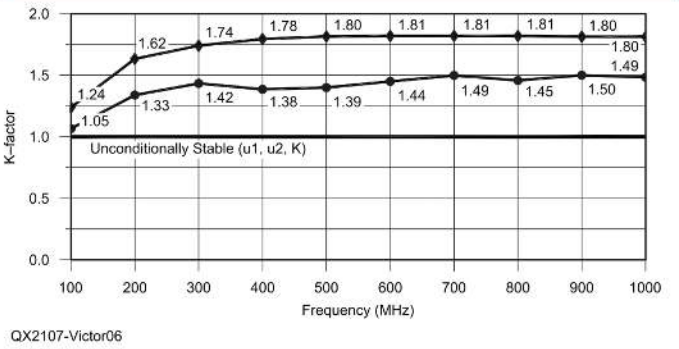

Figure 6 — Model upper trace and measured lower trace K factor based on S-parameters vs. frequency 100 MHz to 1 GHz. A K factor above one is a necessary condition to ensure stability.

device performance **[10]** for a variety of complex impedances. These termination pulls permit the entire range of the Smith chart to be mapped under control of measurement equipment including network analyzers and software. This is beyond the scope of the home lab and the casual construction of RF power amplifiers. However, again the S-parameters provide a reasonable indicator as to the approximate location of the relevant *Z* location. Their application can be leveraged in Class C operation since the load is fixed. This technique is noted in **Figure 7** and discussed next in the section.

Power Amplifier Design

The RF power amplifier operating Class C is efficient and depends on the output current waveform, which is a pulse, while maintaining a near sine wave output voltage. The phase of the output current is ideally maximum when the output voltage is minimum. Thus, the device power dissipation is low. The RF device model illustrates this nicely in operation. Since the input signal is a continuous sine wave of voltage and the output current is a pulse, the device conduction time is short. The Class C amplifier requires no "bias" voltage and depends solely on the input signal to force device operation. The dependence of the amplifier device on input signal level implies operating characteristics are not so straightforward. Simplified statements that the device input impedance is low in Class C bipolar RF power amplifiers is partially correct. However, the magnitude of the input impedance depends on the input signal level. These details are observed in the *Spice* model and determined by running a transient analysis. This transient analysis can be distinguished from the S-parameter analysis as this is a large signal analysis.

Although transient and large signal analysis is the preferred method for the design of RF power amplifiers, it does not preclude the application of scattering parameter information. As discussed earlier, if the amplifier device is stable then a first level estimate is provided by finding the input impedance of the device when terminated by the Class C load resistance discussed in the next section. This input impedance and its region near $Z_{in}(P_o)$ depicted in **Figure 7A** is provided by an input reflection coefficient of the device, Γ_{in}, and the S-parameters, which are those of the device,

$$|\Gamma_{in}| = \left| S_{11} + \frac{S_{12}\, S_{21} \Gamma_L}{1 - S_{22}\, \Gamma_L} \right|.$$

The example case study presented in the next section, for an output power of 1.5 W positions the load reflection coefficient magnitude or $|\Gamma_L|$ near 260 Ω or a value of 0.68. Applying the above $|\Gamma_{in}|$ equation and substituting for Γ_L and converting the reflection coefficient to a parallel equivalent *Z*, reveals an interesting result. Surprising in **Figure 7B** is noticing that the parallel equivalent Z_{in}, represented by an $R_{in} \parallel C_{in}$ from 200 – 600 MHz, lies close to the measurement values for the 2N3866 reported in **[11]**. This demonstrates the utility of small signal parameters to provide some guidance towards large signal operation. Furthermore, it illustrates how areas on the Smith chart dictated by the device scattering parameters can guide termination pulls: load pull and source pull regions. Consequently, I can target the appropriate search regions for proper transistor terminations.

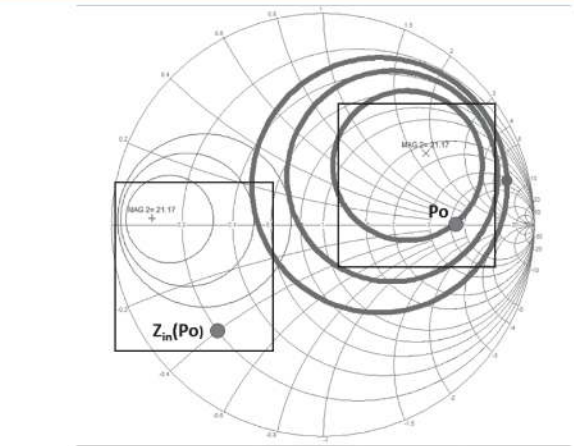

(A)

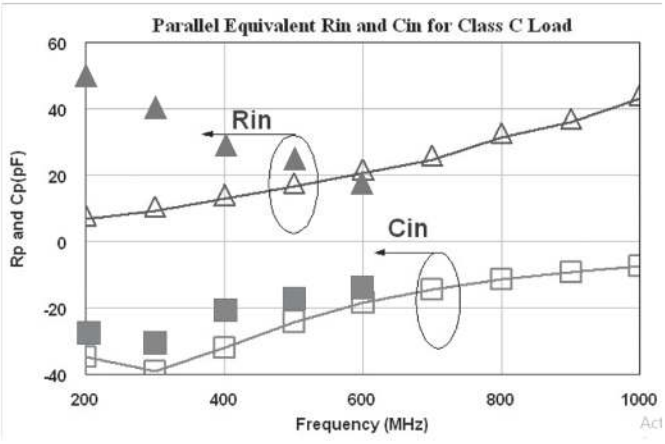

(B)

Figure 7A — Smith chart small signal S-parameters at 200 MHz provide locations for load and source terminations which maximize power gain, GSmax and GLmax. The thin and thick circles are locations of source and load terminations, thick circles providing power gain less than Gmax. Search regions denoted by the rectangular areas guided by the small signal parameters lead to the locations of Po and Zin(Po) suitable for Class C operation. Figure 7B — The parallel equivalent Rin (open triangle) and Cin (open square) from S-parameters with a fixed load of 260 Ω for the Class C termination. The Motorola large signal power amplifier termination specifications are overlaid in solid triangle, Rin and solid square, Cin. The frequency range is 200-to-600 MHz.

Transient Analyses Applied to RF Power Amplifier Operation

Class C RF power amplifiers require a large input signal, which leads to distortion and harmonics. The relationship between input voltage and input current is no longer linear. Since harmonics are present, the voltage and current is distributed among many frequency terms. The Fourier series assists in finding their values. *Spice* provides this information in frequency and the FFT is called upon to find the fundamental voltage and current; both their magnitude and phase. Although the FFT routine is required for large signal evaluation, it does not preclude its application at small signals. This provides an additional check on the model performance and validity. The *Spice* engine has excellent dynamic range, so despite small input signal levels, the fundamental term which will be quite small is easily extracted. The results of the FFT used to obtain the input impedance of the amplifier, Z_{in} is found from,

$$Z_{in} = \frac{V_1 \angle \theta_{v1}}{I_1 \angle \theta_{i1}}$$

where the phase angle of the fundamental voltage and current are reported in the FFT output data. The results obtained when compared to the small signal S-parameter calculation are extremely close. The test setup including bias tees for this exercise is shown in **Figure 8** where a 2N3904 transistor is used at 10 MHz.

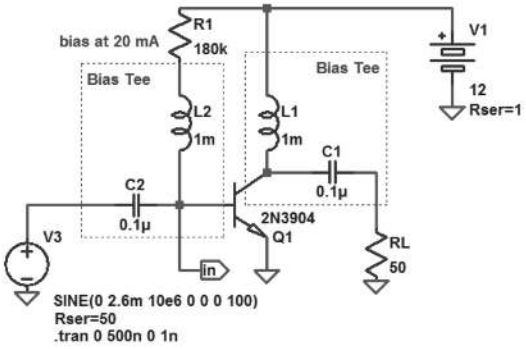

Figure 8 — Nonlinear transient test set is first operated at a small signal excitation level.

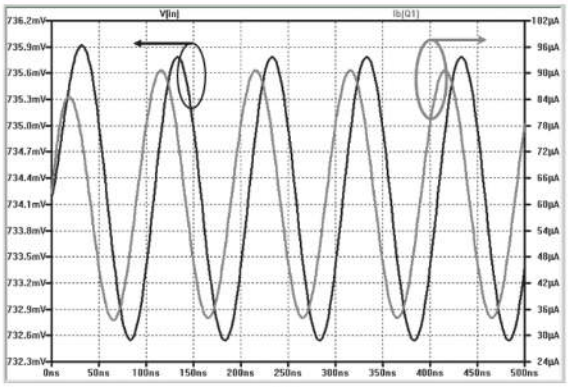

(A)

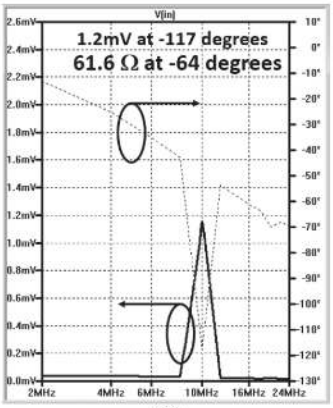

(B)

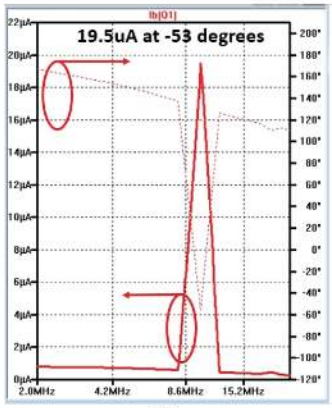

(C)

Figure 9A — Small signal transient solution for the input voltage and current for a 2N3904 at 10 MHz as illustrated in Figure 8. Voltage and current time waveforms in (A) and their resulting transient FFT fundamental base voltage and current in (B) and (C). The resulting Zin matches very closely the S parameter analysis (reflection coefficient) in Figure 10. Note in the time solution in (A), the input current leads the voltage and therefore, the input is capacitive.

A voltage and current solution at the base terminal of the transistor shows the current leading the voltage and the imaginary input Z_{in} component is capacitive. The frequency display of the fundamental voltage and current is shown and the ratio of the voltage and current magnitude and phase result in a Z_{in} of 61.6 Ω with an angle of –64°, **Figures 9A**, **9B** and **9C**. Converting this Z to its real and imaginary parts results in a Z_{in} value of 27Ω real and 55Ω capacitive. This matches the S11 calculated reflection coefficient of the 2N3904 very closely at 10 MHz, 27 Ω real and 55 Ω capacitive, **Figure 10**. Note, Z_{in} from the transient and the FFT output data is 61.6 Ω [cos(–64°) + j sin(–64°)]. For reference, the equation to convert the S11 reflection coefficient to impedance Z_{in} where Z_0 is 50 Ω is:

$$Z_{in} = \frac{1 + S_{11}(V2)}{1 - S_{11}(V2)} Z_0 .$$

Although small signal analysis via the method of transient analysis and FFT is straightforward, it is time consuming to run the analysis and set up the graphs to extract the required data. Small signal analysis is significantly easier within the *Spice* shell using the S-parameter directive mentioned earlier. The real benefit of transient and FFT analysis is when large signal excitation is present. As an example, see the investigation of the dynamic input resistance of the transistor which is mentioned earlier. Although it is usually stated that the input resistance of the bipolar amplifier is low, this is not quite correct. Successive runs in transient analysis for the 2N3866 were done for peak input values of 0.1 through 6 V. The device is biased Class C. A bipolar transistor is essentially **OFF** if the input drive is less than 26 mV, which is the thermal voltage of the device. The input is essentially dominated by a reactance. As the input voltage pushes towards 260 mV, there is a little deflection downward in Z_{in} and there is a clearly defined knee at 500 mV. As the input drive voltage pushes past 500 mV peak, the dramatic decrease in $|Z_{in}|$ is quite apparent, see **Figure 11**.

It is interesting to note that the $|Z_{in}|$ approaches a fairly constant value with further increase in Vin and this value of Z_{in} is not too far removed from the value one would obtain from S11 when Class A operation is used. So if void of any device models for the device selected, one could do an impedance search to maximize power

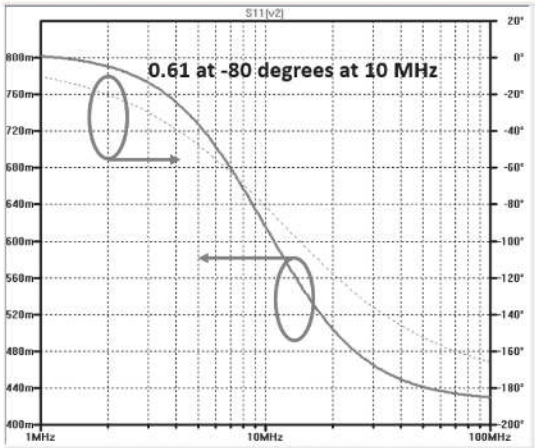

Figure 10 — Small signal S-parameter analysis of the 2N3904 at 10 MHz, 12 V and 20 mA. This reflection coefficient needs to be transformed to its equivalent series Z where Zo is 50 Ω. This is cross checked with the FFTs calculation obtained at a small drive of 2.6 mV as shown in Figure 9.

gain and efficiency based on the S data. The case for maximum power gain is synonymous with finding an input conjugate match point. This facilitates designing an input matching network. Hence, a search around S11*, the conjugate of S11, is useful. While the input is addressed and somewhat complex to get a handle on, the output termination of the Class C power amplifier is constrained. The constraints are the selected supply voltage and maximum permitted current which does not exceed device dissipation and the desired output power. A good estimate for the real part of the load termination is,

$$R_L = \frac{Vcc^2}{2P_o}.$$

Finding the value of Z_{in} for the amplifier is now easy. First, terminate the collector in R_L and then drive the input voltage to a value providing the desired P_o and power gain, G_p. The case cited in the prior section is obtained for a V_{cc} of 28 V and an output power of 1.5 W. This has been done for the 2N3866 and has been published as a reference document by Motorola, AN-282 **[11]**. In this document, the disparity between small signal S-parameters and high power impedance values are highlighted for a wide range of devices. The output powers cited ranged from 1 W to 50 W. This reference document is used to benchmark the technique discussed here and includes data for the 2N3866.

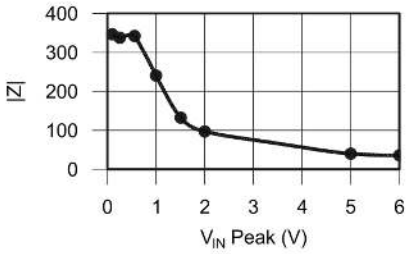

Figure 11 — Input |Z| vs. increasing peak drive voltage at the base.

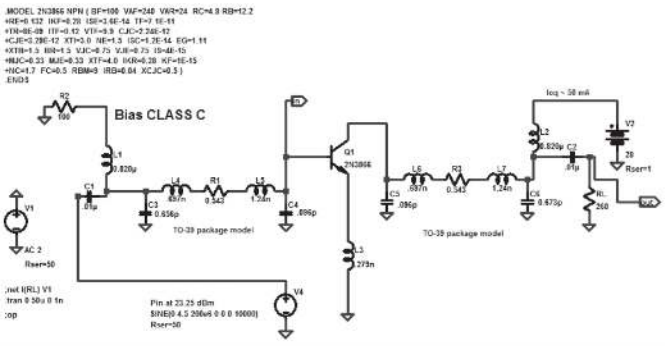

Figure 12 — Device 2N3866 with TO-32 package and Class C bias. The load is set to 260 Ω.

Large Signal Amplifier Design / Class C

The supply voltage selected is 28 V and the lowest frequency with comparative data from **[11]** is 200 MHz. Output power data curves between 1 W and 1.5 W are available and they cited the parallel equivalent input resistance and capacitance vs. frequency. The real part of the output impedance is constrained by the desire to have the collector swing twice the supply voltage and provide the desired output power, 1 to 1.5 W. This dictates a value for R_L between 260 and 390 Ω. A 260 Ω load is used in the test set, see **Figure 2**. The input signal is provided by a voltage source with a generator resistance of 50 Ω. The source power peak voltage is adjusted in model simulation until the output power is 1.5 W. The simulation network is shown in **Figure 12**. The resulting large signal input voltage and current are shown in **Figure 13A**, and fundamental FFTs of V_1 and I_1 are in **Figure 13B** and **Figure 13C**. **Figure 13A** demonstrates the capacitive input as the current leads the voltage. The fundamental ratio for Z_{in} is expressed in parallel form by dividing the $|Z_{in}|$ by the cosine and sine of the difference angles given in **Figure 13B** and **Figure 13C**, –228°. This angle is corrected to the proper rectangular impedance quadrant. This is accomplished

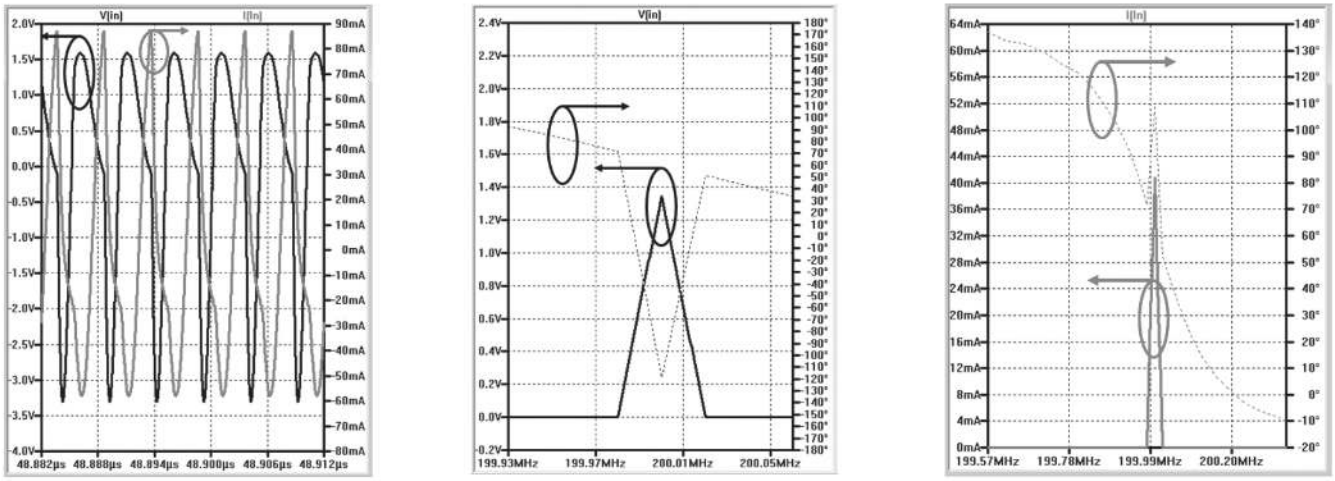

Figure 13A — The input voltage and current large signal response and Zin is obtained from the FFT of the model in Figure 12. Note the current leads the voltage. The resulting Zin is 34 Ω and –48°. Hence the parallel equivalent Zin is 50.8 Ω || –j45.8 Ω, or 17.4pF 200 MHz. Figure 13B — FFT input voltage and phase. Figure 13C — FFT input current.

by adding 180° to the resulting angle. The resulting angle is –48° and therefore capacitive. Hence, the real parallel R input is 1/cos(–48°) or 1.49×(1.4 V / 41 mA) or 51 Ω and the parallel reactance is capacitive 1/sin(–48°) or, –1.35×(1.4 V / 41 mA) or 17 pF at 200 MHz. The real part of Z_{in} compares favorably to the results in **[11]** at 50 Ω. While the parallel capacitance is 17 pF and not 32 pF, there is no mention in the note addressing fixture capacitance. It is suspected that a portion of the reported 32 pF is due to additional stray parasitic capacitance of the fixture.

The Breadboard Response

The complex input impedance, Z_{in}, is derived from the FFT response for a large signal input power of 23 dBm. The real part of the load is set for Class C operation based on swinging the collector voltage by twice the supply. The FFT routine is also applied at the output and determines the imaginary part of the output impedance. The result returns 3 pF at 200 MHz which is nearly the equivalent shunt C obtained from S22 of 2.4 pF. The results for Z_{in} and Z_{out} are now determined as

$$Z_{in} = 51\Omega \,||\, 17\text{pF}$$

$$Z_{out} = 260\Omega \,||\, 3\text{pF}\,.$$

A set of Pi networks are chosen to transform the 50 Ω source and load to Z_{in} and Z_{out}. A Q of 4 is chosen for the input side and a Q of 10 for the output. Component values are chosen partly from what is available and what would be reasonably free of parasitic effects at 200 MHz. The parasitic problems are in themselves a challenge and must include component losses. The initial values for the Pi network ranged from 39 to 70 pF and the inductors from 20 to 30 nH. While the inductors were reasonable in size, the capacitors with their lead lengths were not. The capacitor lead lengths and resulting inductance from the component to component connections increases the value of the capacitor. The resulting amplifier response centered around 150 MHz, however it displayed a power gain of nearly 14 dB at 1 W power output with 17 dBm input power, the maximum level available from the test equipment at hand. The dc conversion efficiency measured 64%. Adjustment of the Pi networks can easily be done with a SWR bridge or a directional coupler. First construct the Pi network only and terminate it into the desired parallel impedance. Then adjust component values seeking a return loss of 20 dB or better over the desired band. The results for the amplifier gain response is shown in **Figure 14** and the input and output match response in **Figure 15A** and **Figure 15B**. The dc conversion efficiency over the passband dictated by the output Pi-network Q is 60%.

The Class C power amplifier required a minimum of 20 dBm to attain an output of 1 W to 1.5 W. The model assisted in verifying the reduction of output power at 200 MHz with 17 dBm input power. This is key. The beauty of model availability and tools which can handle a large signal nonlinear response network are important assets in understanding why circuits behave as they do. As an example, component losses or their Q should be added to the model simulation. The approach outlined here should be applicable to Class C designs for other devices such as MOSFETS, IGFETs and larger bipolar devices.

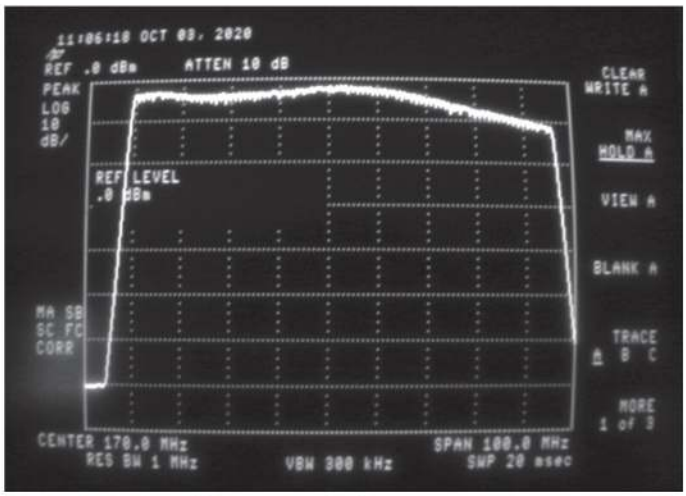

Figure 14 — Amplifier power gain frequency response. The supply voltage is 28 V and the conversion efficiency is approximately 60% at band center. Top scale is 30 dBm (1 W). Pin is 17 dBm. Center frequency is 170 MHz; frequency span is 100 MHz.

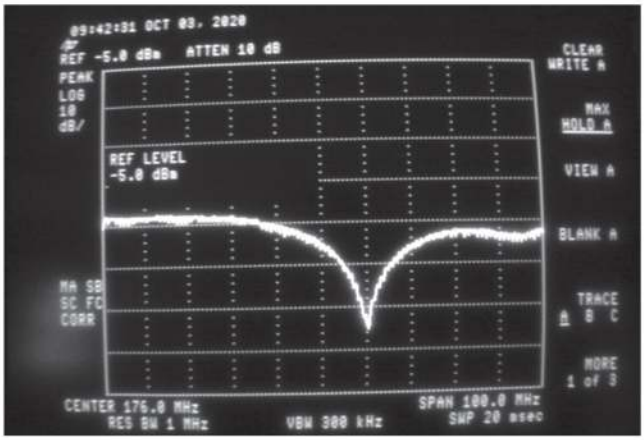

(A)

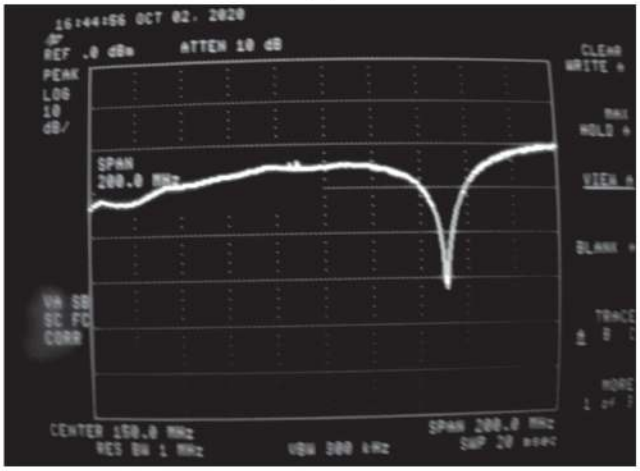

(B)

Figure 15A — The measured amplifier input return loss versus frequency at 17 dBm input power. The reference top level is 0 dB at 3 divisions down from the top 5 dB/division. Near the amplifier center frequency return loss is better than 15 dB. Figure 15B — The measured amplifier output return loss versus frequency at 17 dBm input power. The reference top level is 0 dB at 1 division down from the top, 10 dB/division. Near the amplifier center frequency return loss is better than 15 dB.

Conclusions

An approach to the design of Class C RF power amplifiers was presented. *Spice* models were validated by using measured S-parameter data. The *Spice* model supported transient operation and the application of the FFT within *Spice* extracted the complex input and output impedances under actual operating conditions. These data points, namely large signal Z_{in} and Z_{out}, if not provided by the manufacturer, which are key to RF power amplifier design, can be supplemented by other techniques. In the absence of a model or large signal impedance, the device small signal parameters do provide a direction for searching and minimizing guess work to achieve a successful design.

Alan Victor, W4AMV, was licensed in 1964. He operates mostly CW using an all homebrew station and enjoys design, construction and restoration of communication and test equipment. Alan worked in both the communication and semiconductor engineering fields. He received his PhD in electrical engineering from North Carolina State University and is currently involved with their mentorship program assisting new graduates in their engineering studies.

References

[1] P. W. Tuinenga, *SPICE A Guide to Circuit Simulation & Analysis Using PSpice*, Prentice Hall, 1988.
[2] A. Vladimirescu, *The Spice Book*, John Wiley & Sons, 1994.
[3] G. Gonzalez, *Microwave Transistor Amplifiers*, pp.453, Prentice Hall, 1997.
[4] Spice Model available at: **https://www.analog.com/en/design-center/design-tools-and-calculators/ltspice-simulator.html**.
[5] P. Kopyt, D. Gryglewski, W. Wojtasiak, W. Gwarek, "Electrical Characterization of a Wirebond TO-39 Package for IR Radiation Detectors," MIKON 2012, pp.213-216.
[6] R. S. Carson, *High-Frequency Amplifiers*, John Wiley & Sons, pp. 13-16, 1975.
[7] *Motorola Semiconductor Technical Data, MRF3866R2*, Rev 7, Q1/96.
[8] *LTSpice*, **www.analog.com/en/design-center**.
[9] *AppCAD* Version 4.0.0: **www.hp.woodshot.com**.
[10] M. Hiebel, *Fundamentals of Vector Network Analysis*, Rohde & Schwarz GmbH &Co., 2008, pp. 288-336, Chapter 7, "Nonlinear Measurements, "see section 7.8 "Load-pull measurements."
[11] R. Hejall, *Systemizing RF Power Amplifier Design*, AN-282 Application Note. An abbreviated note is available at: **https://www.nxp.com/docs/en/application-note/AN282A.pdf**.

Letters

Protocol for Formatting and Transmitting Binary Data over Morse CW (May/June 2021)

Dear Editor,

I found the Brian Callahan, AD2BA, article very interesting. The general approach seems useful. Based on my experience, sending binary data blocks from Arduino to PC with no hardware handshake, I think that relying on the spacing between blocks of data is risky. I have gone to using markers, which cannot be data, similar to the Motorola format. Also, I favor human debugging over speed, so I propose a different set of characters:

Ø=O, 1=E, 2=I, 3=A, 4=H, 5=5, 6=X, 7=V, 8=K, 9=N, A=A, B=B, C=C, D=D, E=Y, F=F, also a marker, something like zero, which is easy for humans and machines.

My proposed encoding is 16% slower than the way I interpret that in Callahan's table if we ignore spaces between characters and assume a random distribution of digits. If digits follow the Newcomb-Benford law, it is probably slower by a similar amount, since Callahan's low digits are also shorter codes. — *Best regards, David Underwood, KØIMH*; **sealions@earthlink.net**.

The author responds

As someone who has been working on free Unix operating systems for nearly a decade, I appreciate the desire for human debug-ability and the avoidance of the risky. Admittedly, I may have perhaps left both a little too much to the stations in my baseline CW Record Protocol formulation.

A marker between records may well be wise; we could even go so far as assigning a new AX prefix to data records without separation and reassign A0 to data records with separation, with A1 termination records not needing a termination character. Or perhaps, similar to both Intel and Motorola, the separation character may be the prefix, avoiding the need for anything more in the specification than a remark that records may begin with five dahs (Ø) to increase legibility.

When devising the example encoding for the article, I made a point to avoid the longer characters. I still believe that avoidance of long characters can be useful when both stations are human. Otherwise, though a 16% slower encoding would certainly be felt, it may not be of too much significance. I appreciate your letter, giving me ideas for expansion of the protocol. — *Best regards, Brian Robert Callahan, PhD, AD2BA;* **callab5@rpi.edu**.

Thoughts on Amplifier Output Impedance (May/June 2021)

Hello Maynard,

Thanks for the illuminating article (Maynard A. Wright, W6PAP, in May/June 2021 *QEX*) on amplifier output impedance. You reached the right conclusion. An amplifier's Thévenin equivalent source impedance is not equal to the amplifier's load impedance, nor its conjugate. Thévenin impedance does not tell anything about dissipation inside a "black box" Thévenin source. In particular, one should not infer efficiency from a Thévenin impedance. Efficiency computation requires knowing the internal structure and performing circuit analysis. *EDA* software for circuit design refers to numerical determination of amplifier output impedance as "hot S11" calculation. Programs like *Microwave Office* and *Keysight ADS* are routinely used for amplifier design and do such calculations correctly. Solid-state amplifiers are designed for gain, noise, and stability over a range of admissible load impedances. Design trades can be understood using various circles on a Smith chart. Conjugate matching is a red herring and may lead to instability or poor noise performance, and is not a valid criterion for amplifier design. I am glad you set the record straight. — *73, Steve Stearns, K6OIK; Saratoga, CA.*

The author responds

Hi Steve,

Thank you for your kind words. They mean a lot coming from such a gifted author. I especially benefited from "Crest Factor of Sinusoidal Electromagnetic Fields," (*QEX*, July/August, 2020) as I would have had no idea that the ratio could deviate from $\sqrt{2}$ without your explanation. — *73, Maynard Wright, W6PAP; Citrus Heights, CA.*

Send your *QEX* Letter to the Editor, via email to qex@arrl.org. We reserve the right to edit your letter for clarity, and to fit in the available page space. *QEX* Letters may also appear in other ARRL media. The publishers of *QEX* assume no responsibilities for statements made by correspondents.

Richard (Ric) A. Tell, K5UJU

Richard Tell Associates, Inc., 10037 Long Meadow Rd., Madison, AL 35756; **rtell@radhaz.com**

Amateur Portable Radios (Handheld Transceivers): Exposure Considerations Based on SAR

New FCC rules related to human exposure that went into effect on May 3, 2021 may now potentially require compliance with limits on specific absorption rate.

Introduction

In what might have been unnoticed by most hams, the FCC has instituted new rules related to human exposure that went into effect on May 3, 2021 that may now potentially require compliance with limits on specific absorption rate (SAR) **[1]**. This new rule, among others, is a part of what is called the FCC's *ET Docket No. 19-226* that changes the way that parties determine and achieve compliance with the Commission's limits on human exposure **[2]**. Of special interest to amateur radio licensees, the new rules no longer necessarily exempt handheld transceivers (handhelds) used by hams from certification that their use will comply with an SAR limit, something that historically has always been a requirement for commercial handhelds — those used outside the amateur radio service.

According to the FCC announcement, it appears that the commission intends to grandfather any equipment that was presumed to be compliant prior to the May 3 date. Since amateur radio equipment has never been required to be certified as to performance, except for certain power amplifiers, it seems reasonable to assume that all existing handhelds, the focus of this article, would remain designated as compliant devices. Nonetheless, new handhelds purchased after the effective date would presumably need to become certified, but any SAR testing, if mandatory by the FCC, might conceptually only become required after some to-be-determined review period. The most likely scenario is that, going forward, manufacturers will be required to evaluate SAR for amateur radio handhelds. In summary, amateurs are no longer relieved from compliance with FCC RF exposure rules by exception. Rather the amateur service will now be treated similar to all of the other services regulated by the FCC.

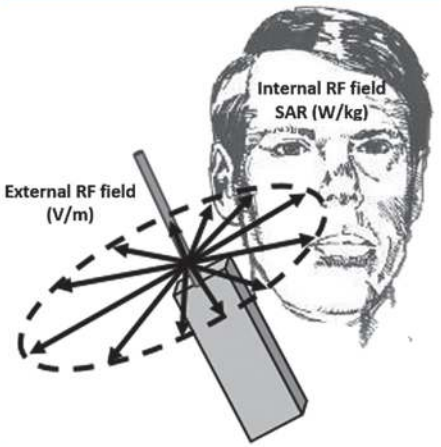

Figure 1 — RF electric and magnetic fields external to the body result in internal electric fields that can produce tissue heating based on the specific absorption rate (SAR).

Aside from the question of exactly when operation of a particular handheld is expected to comply with the new rules, the whole matter of SAR and how it relates to exposure of the user and others nearby is a complex subject and generally not familiar to most hams. Indeed, the assessment of SAR itself is beyond the capability of the vast majority of licensees. This article helps provide a basic understanding of what SAR is all about and how it relates to the safety of operating equipment, whether handheld of not, that produces radio frequency (RF) fields. The following presents 1) a simplified explanation of SAR to help in appreciating the complexity of the new FCC requirements as they may relate to controlling SAR and, 2) insight as to the likely SARs that might result from use of amateur handhelds.

Background

Fundamentally, RF fields interact with objects in an environment, often inducing RF currents to flow in those objects. If the exposed object is composed of a lossy (absorptive) material, such as human tissue, the induced currents largely lead to heating. If the heating effect is sufficiently robust, associated with very intense RF field strengths, there may be an increase in the temperature of the exposed tissues. Hence, tissue heating is directly related to the

strength of the electric field strength within the tissue. The preferred way to quantify this internal heating effect is a quantity called the SAR expressed by the unit watt per kilogram (W/kg) of tissue. SAR expresses the rate at which an electromagnetic field delivers energy to the subject tissue. SAR is an expression of energy absorption rate because power is the time derivative of energy; 1 W is equivalent to 1 J/s. Thus, an SAR of 1 W/kg is equivalent to an energy absorption rate of 1 J/kg·s.

RF electric and magnetic fields external to the body result in internal electric fields that can produce tissue heating based on the SAR, see **Figure 1**.

SAR limits for safe exposure

The FCC RF exposure limits are based on limiting the SAR averaged over the whole body and as averaged over any one gram of tissue. These limits are designed to protect against increases in core temperature of the body and of localized regions of tissue that might result in an adverse health effect. For amateur radio licensees, members of the licensee's household and persons who are occupationally exposed to RF fields, the whole body SAR limit is set at 0.4 W/kg (averaged over the entire body mass) and a local (spatial maximum) SAR limit of 8 W/kg (averaged over any single gram of tissue in the body). For members of the general population (all persons who are not amateur licensees or occupationally exposed), the corresponding SAR values are 0.08 W/kg whole body and a local value of 1.6 W/kg. The FCC RF exposure limits specify maximum permissible exposure (MPE) values of RF fields that exist outside the body that are expressed as values of electric (E) field strength (V/m) and magnetic (H) field strength (A/m) as well as power density (W/m^2 or mW/cm^2). Compliance with the MPEs is intended to ensure that the whole body SAR and local SAR limits within the body are always respected and, clearly, electric and magnetic field strengths in air are much easier to measure (and calculate) than those values inside the body. Because cell phones are used by the general population with no particular expectation they may be exposed to RF fields, the applicable limit is the more stringent SAR value of 1.6 W/kg. Handhelds used in commercial activities must comply with the less restrictive limit of 8 W/kg.

It should be noted that the FCC in the US references the limit for local SAR to an average over a one gram cube of tissue. The recommended local SAR limit developed by the Institute of Electrical and Electronics Engineers (IEEE) in their *IEEE Std™ C95.1-2019* specifies a larger averaging tissue mass of 10 g in the shape of a cube **[3]**. This greater averaging mass has been found to better correlate local tissue temperature increase with local SAR. This same larger averaging mass is also specified in the International Commission on Non-ionizing Radiation Protection (ICNIRP) guidelines widely applied in Europe **[4]**. More about this later.

For RF sources that are sufficiently far from the body, MPE values accurately correlate with SAR. A complicating factor, however, is that a measurement of the E or H fields (or power density) outside the body does not necessarily accurately correlate with the local SAR in tissue *when the RF source is extremely close to the body surface*. This is why the FCC requires all commercially used handhelds including cell phones to be evaluated on the basis of local SAR, not MPE, before they are allowed to be sold in the US. As might be suspected, for cell phones as well as handhelds, the greatest SAR in the body is usually at the point where the transmitter is positioned. This might be the ear in the case of a cell phone or the front of the face in the case of a handheld. During SAR measurements, the transmitter is positioned either in direct contact with the head or other part of the body such as when cell phones or handhelds are mounted at the waist. When test laboratories evaluate SAR for common handheld use, the handheld is positioned at typically 2.5 cm in front of the face, similar to when the handheld is held in front of the mouth. A specially shaped phantom is often used for laboratory measurements of SAR, the phantom being similar to a manikin filled with a material that simulates the RF absorption characteristics of human tissue. Cell phone and commercial handheld manufacturers must commit to these detailed laboratory measurements for every model of their RF emitting product, revealing the maximum local SAR that can result when the device is operating normally at its maximum rated power. This has led to a gigantic database of equipment certifications resident in the FCC's equipment authorization database **[5]**. In each testing case, the product is placed in appropriate positions relative to the phantom while miniature probes are robotically moved throughout the interior of the phantom to measure the E field strength. Based on the measured E field in the phantom and the conductivity of the tissue equivalent material filling the phantom, the SAR is determined. See the **Sidebar: Determining SAR**.

Determining SAR

SAR can also be determined through theoretical analysis but, in practice, cell phones and commercial handhelds are always evaluated for SAR using the described laboratory procedures. The analysis approach makes use of the so-called finite difference time domain (FDTD) method, a complex computer based computation wherein the human body is modeled by breaking it into a very large number of small voxels — typically measuring one or two mm on a side — each with an assigned set of electrical properties to mimic the electrical characteristics of human tissues. The computations can take hours to run on super-fast machines with the output data ultimately processed to display local SAR values in a three dimensional fashion.

A challenge for amateur radio licensees

Fortunately, this SAR evaluation process has never before been required for equipment used in the amateur radio service, which can lead to increased costs of equipment. It remains to be seen how these new FCC rules will impact the certification of amateur radio handhelds for conformance with the local SAR limit. Just as important, though, is the matter of how amateur radio operators would be able to conclude that their use of a ham handheld complies with the relevant SAR limits for the equipment that they currently operate.

Confronted with this challenge, an alternative but practical approach to assessing compliance of amateur radio handhelds against the fundamental exposure criterion of SAR is required. This paper suggests that, at this point in time and supported by the extensive database of equipment certifications available from the FCC, most amateur radio handhelds already can be expected to comply with local SAR values that underlie the FCC RF exposure rules. For example, the FCC's equipment authorization database represents more than two decades worth of detailed, time consuming and expensive SAR test results for cell phones and commercially

used handhelds as well as for all kinds of other RF emitting devices that may be used close to the body. It is proposed that this extensive set of SAR certification data can be used to amateur radio's advantage. Of particular interest are the many reports filed in the database on commercial handhelds that operate in frequency bands that are extremely close to — or, in some cases, actually within — those authorized for the amateur service. Fortunately, there are several bands allocated for commercial communications that are essentially similar to those used by hams in the VHF and UHF spectrum. For example, the US amateur bands at 2 m (144-148 MHz), 1.25 m (219-225 MHz), 70 cm (420-450 MHz) and 33 cm (902-928 MHz) are frequency allocations very close to those used for commercial communications activities and for which SAR evaluations have been conducted.

By examining SAR measurement results for commercial handhelds operated in these close-by frequency bands, significant insight can be gleaned on the likelihood of compliance of similar amateur radio handhelds despite the fact that the amateur versions of these radios have not necessarily been directly measured for SAR. For instance, say that 2 W commercial handhelds that operate just below and just above the two-meter band are found to comply with the SAR limit. It would seemingly be reasonable to conclude that a 2 W amateur handheld that operates in the two-meter band would also be found to be similarly compliant.

A practical example

To help illustrate this concept, an example search of the FCC equipment authorization database was conducted of a limited number of SAR certifications; the sheer size of the database begs the question of how much effort would be required to query every certification to determine its relevance to VHF/UHF handheld compliance. Ideally, some sort of automated process would be very helpful in sorting through the thousands of reports but that remains to be determined, if feasible, by the FCC. The manual approach to searching the database and extracting relevant SAR data, while extremely time consuming, can, nonetheless, result in helpful insights.

Of great utility, virtually all of the SAR certifications of commercial handhelds contained in the FCC database include the results of SAR measurements averaged over both the FCC's 1 g averaging mass as well as a 10 g averaging mass applicable to most markets outside the US. **Figure 2** for 1-gram averaging mass, and **Figure 3** for 10-gram averaging mass illustrate the results of an initial and limited inspection of the FCC's database for SAR certifications of commercially used handhelds across the VHF/UHF spectrum for compliance with the FCC limits. The indicated local SAR values retrieved from SAR reports have been normalized to 1 W and are relative to a duty cycle of 50% based on the push-to-talk (PTT) operation of the handheld. For compliance determination purposes, the FCC applies a presumed duty cycle of 50% for PTT operation of the handheld.

Figure 2 shows the local one-gram averaged SAR produced by commercial handhelds that operate near or within amateur radio bands (based on 50% PTT duty cycle and 1 watt). These data are potentially applicable to US amateurs regulated by the FCC should the FCC require compliance with SAR limits.

Of particular note is the lower normalized local SARs associated with VHF handhelds as opposed to those used in the UHF range; the higher frequencies result in a shorter depth of penetration resulting in higher surface region SARs. Also apparent from the data in **Figure 2** is the relatively wide margin by which the VHF local SARs

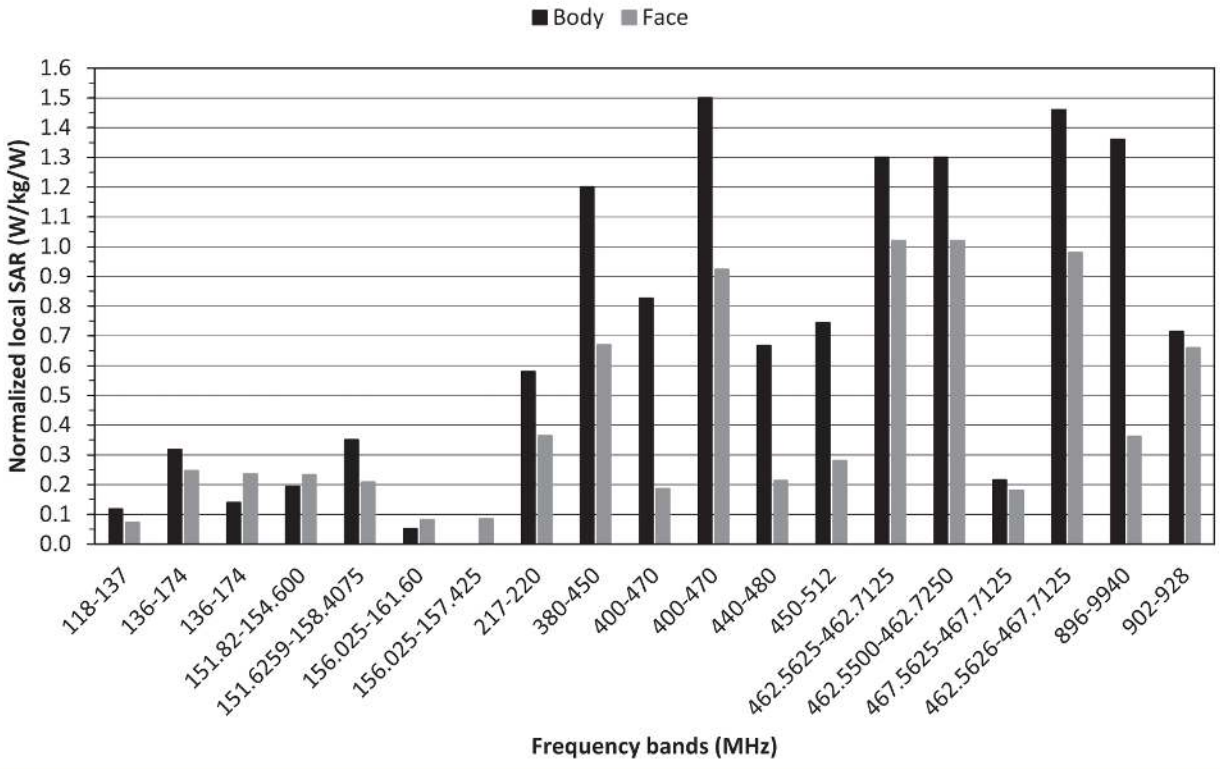

Figure 2 — Local one-gram averaged SAR produced by commercial handhelds that operate near or within amateur radio bands (based on 50% PTT duty cycle and 1 watt).

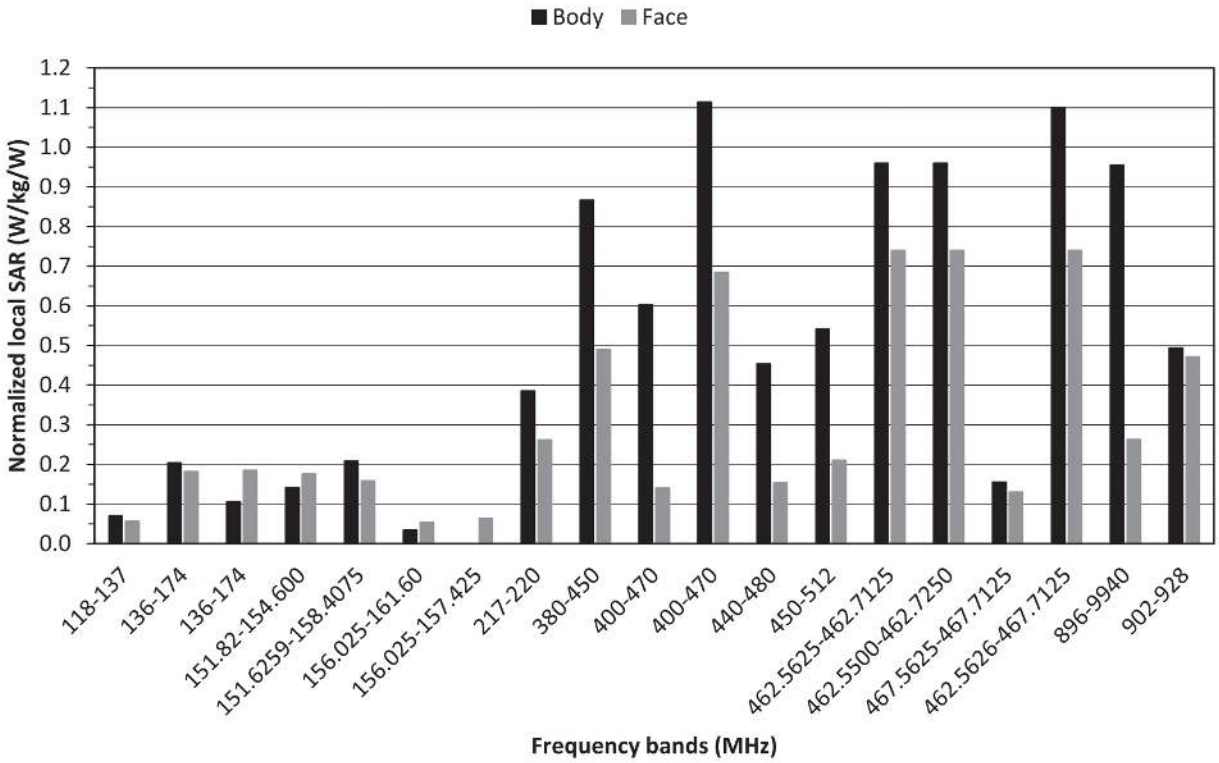

Figure 3 — Local ten-gram averaged SAR produced by commercial handhelds that operate near or within amateur radio bands (based on 50% PTT duty cycle and 1 watt).

comply with the more stringent local SAR required for devices used by the general population, i.e., 1.6 W/kg. The FCC applies the occupational MPEs (and by association, a higher local SAR limit, i.e., 8 W/kg) to amateur radio operators and members of their households. In the US, the application of occupational limits to hams is based on the presumption by the FCC that licensed radio operators have a basic awareness of their potential exposure and are knowledgeable of how to prevent excessive, unsafe exposures.

A practical application of **Figure 2** is the extrapolation of the normalized local SARs to a local SAR of 8 W/kg (the FCC limit for amateurs) to determine the power level that would result in 8 W/kg. For example, in the 2 m band, it might be presumed that an handheld operating with a power of up to 22.9 W (not realistic for an handheld) could be used before exceeding the amateur radio operator SAR limit (8 W/kg divided by 0.35 W/kg/W). For a 70 cm handheld, a power of 5.3 W could be used that would just comply with the local SAR limit (8 W/kg divided by 1.5 W/kg/W).

A similar display of normalized local SAR based on an averaging mass of 10 g, rather than just 1 g, is provided in **Figure 3**. It shows the local ten-gram averaged SAR produced by commercial handhelds that operate near or within amateur radio bands (based on 50% PTT duty cycle and 1 W). These data are potentially applicable to amateurs subject to regulations based on SAR limits as specified by ICNIRP. Whether regulatory agencies in countries other than the US presume a PTT duty cycle of 50% is not certain.

The same attribute of relatively lower local SAR for VHF handhelds is apparent, but the actual normalized values are less than those that would result from the smaller averaging mass of 1 g. This characteristic results from the greater volume of tissue over which highly localized points of SAR within tissue may be averaged. The practical upside of this is, obviously, that 10 g averaging allows for higher handheld operating powers.

It is also noteworthy that there is a variation in the normalized SAR values,

Work in progress

In the US, the American Radio Relay League (ARRL) is working diligently toward development of guidance to amateurs to help in their compliance efforts in view of the new FCC RF rules. In this context, the ARRL RF Safety Committee, chaired by Dr. Gregory Lapin, N9GL, (email: **n9gl@arrl.org**) is monitoring the new regulatory requirements that are applicable to the amateur radio service and working to develop appropriate methods to help hams in their compliance efforts.

Simultaneously, a small group of UK amateurs in the Radio Society of Great Britain (RSGB) and the ARRL in the US have been convening since mid-2020 to collaboratively attack the same issue, i.e., how amateurs can best assert and/or demonstrate compliance with the proposed new RF rules to be administered by Ofcom in the UK and the new changes in how the FCC rules are being applied to hams in the US. For more information on this activity, see articles in *RadCom* from the RSGB or contact John Rogers, MØJAV (email: **m0jav@rsgb.org.uk**).

sometimes among different handhelds that operate in an identical frequency band. This is likely to reflect differences in the antennas or other accessories that may be used with the specific radios.

For hams outside the US who must comply with ICNIRP guidelines, assessing compliance would be based on applying the 10 g averaging mass and on somewhat greater SAR values. For instance, the ICNIRP local SAR limit for occupational exposure is 10 W/kg as compared to the FCC's 8 W/kg while the local limit for the general public is 2 W/kg compared to the FCC's 1.6 W/kg. Hence, the normalized SARs shown in **Figure 3** should be extrapolated to a value of 10 W/kg for estimating the maximum handheld power that would comply with the ICNIRP occupational SAR limits. This results in greater permissible handheld powers than could be permitted with the smaller averaging mass specified by the FCC. Two competing factors are potentially relevant to the handheld compliance issue where exposure limits are based on ICNIRP. First is whether hams are considered as members of the general public or whether they are treated as occupationally exposed workers, the public exposure limits being a factor of five more stringent. Second, the greater local SAR averaging mass would help mitigate against noncompliance.

Irregular ham Handheld configurations and SAR

When reviewing the SAR certification reports in the FCC database, it is evident that the SAR testing procedures can become rather onerous. This is reflected in the multiple configurations of an handheld with different antennas, battery packs and other accessories such as microphones and headsets that are each individually evaluated for many commercial handhelds. From a ham's perspective, however, this extensive testing process for commercial handhelds would seem to help support an argument that common amateur use of third-party accessories such as higher gain antennas, etc., will not materially change the rather clear conclusion that ham handhelds would continue to comply with exposure rules requiring assessment of SAR. Of particular relevance, for the handhelds identified in this limited exercise, a variety of antenna lengths were found to have often been included in the tests. The results plotted in **Figures 2** and **3** encompass the absolute maximum reported local SARs for each handheld, regardless of a particular accessory, in the interest of conservatism. An important principal, relative to local SAR associated with handhelds, is the physical size of the antenna; for a given power, contrary to how gain is generally proportional to antenna size, smaller antennas result in a higher concentration of energy absorption. For hams, replacement of antennas on handhelds to improve potential coverage is most often accomplished with larger, longer antennas. This fundamental relationship between antenna size and local SAR likely means that using third-party antennas on handhelds results in lower SARs.

Conclusions

A careful but limited examination of SAR test results available in the FCC's equipment authorization database suggests that handhelds commonly used in the amateur radio service would not exceed exposure regulations based on the magnitude of local SARs. This tentative conclusion could be used to support an amateur radio operator's contention that their past use of existing handhelds as well as acquisition and use of new handhelds complies and will be expected to comply with possible SAR based exposure regulations. Extension of this initial data analysis is recommended to further clarify this conclusion. Operation of relatively higher power handhelds could result in exceeding local SAR limits for members of the general population and care should be exercised in permitting unlicensed persons to use such handhelds even under the supervision of a licensed control operator. See the **Sidebar: Work in progress**.

Outside the jurisdiction of the FCC, Ofcom in the UK has announced that it will impose new license requirements for UK hams that are based on the ICNIRP guidelines. The RSGB has developed useful information on this upcoming requirement **[6]**. At this time, however, it remains to be seen exactly how such new regulations might impact UK hams. Interestingly, Ofcom is only concerned with radio operations that cause exposure of the general public, not with the potential exposure of hams themselves. However, Public Health England and/or the UK Health and Safety Executive, separate government entities in the UK, could recommend RF exposure limits that might include exposure limits for hams. Whether any of the possible regulatory provisions in the UK would apply the more permissive exposure limits for occupational exposure to amateur radio operators, similar to the FCC, or the more restrictive limits applicable to the general public, is unknown.

Ric Tell, K5UJU, received his Novice ticket in 1959, first operating with a home brew 7.5 W transmitter during the greatest solar cycle of his life. Eventually achieving an Amateur Extra class license in 1970, his predominant activities have included his professional pursuits in the areas of RF safety, RF instrumentation, antenna analysis, hazard assessments and compliance evaluations. After spending 20 years with the Environmental Protection Agency, he has operated his own scientific consulting business since 1987. His ham radio interests are primarily QRP CW operation and experimenting with antennas. He holds a BS degree in physics and an MS degree in radiation sciences and is a member of the ARRL RF Safety Committee and is a Life Fellow of the IEEE. Ric chairs the IEEE Committee on Man and Radiation (COMAR) and Subcommittee 2 on RF safety programs in the IEEE International Committee on Electromagnetic Safety, Technical Committee 95.

References

[1] *FCC Public Notice.* Office of Engineering and Technology announces May 3, 2021 as the effective date for RF exposure rule changes and beginning of the two-year review period for existing parties. Available at: **https://docs.fcc.gov/public/attachments/DA-21-363A1.pdf**.

[2] *Human Exposure to Radiofrequency Electromagnetic Fields and Reassessment of FCC Radiofrequency Exposure Limits and Policies.* Final rule. Federal Register, Vol. 85, No. 63, Wed., April 1, 2020, pp. 18132-18151. Available at: **https://www.govinfo.gov/content/pkg/FR-2020-04-01/pdf/2020-02745.pdf**.

[3] *IEEE (2019). IEEE Standard for Safety Levels with Respect to Human Exposure to Electric, Magnetic, and Electromagnetic Fields, 0 Hz to 300 GHz.* IEEE Std C95.1-2019. Available at: **https://ieeexplore.ieee.org/browse/standards/get-program/page/series?id=82**.

[4] *ICNIRP (2020). Guidelines for limiting exposure to electromagnetic fields (100 kHz to 300 GHz). Health Physics*, Vol. 118, No. 5, pp. 483-524. Available at: **https://www.icnirp.org/en/publications/article/rf-guidelines-2020.html**.

[5] FCC equipment authorization database at: **https://apps.fcc.gov/oetcf/eas/reports/GenericSearch.cfm**.

[6] *EM Field Exposure. Radio Society of Great Britain (RSGB).* Available at: **https://rsgb.org/main/technical/emc/emf-exposure/**.

Jacek Pawlowski, SP3L

Drzonkow – Krucza 6, 66-004 Zielona Gora, Poland; **sp3l@wp.pl**

Designing Antenna Systems for Low Common Mode Current in Coaxial Feed Lines

With antenna simulation programs you can reveal common-mode current problems and reduce them while still in the design phase.

I once built an antenna that did not work as the computer simulation had predicted. The antenna was heavily unbalanced with one arm much longer than the other one, so it was not difficult to identify the main suspect — large common-mode current (CMC) on the coax feeder shield detuned the antenna and changed its radiation pattern. I had used a common-mode choke wound on a ferrite core from the very beginning and even later added an additional air-wound choke in series with the first one but it did not help. I had no choice. It was time to study the CMC related publications in depth. I read whatever I could find on the internet, including various books and catalogs. I realized that I needed to write down the things I had learned and organize this information in a logical way. That was the origin of this article. Except for the information I found in the other publications, I added to the paper my own conclusions resulting from many hours of simulations and calculations. My goal was to understand how the CMC is excited on the coax shield and how one can calculate its value using antenna simulation programs. I realized that with the addition of some figures, this paper might be helpful to other antenna designers.

Standard Way of Modeling Antennas

Most antenna models created for computer simulations neglect the presence of the coax feeder and its impact on antenna performance. Let's consider the simplest case: a horizontal dipole. A typical model of this antenna consists of just a source and two equal length legs (**Figure 1A**). The hidden assumption in this model is that the impact of the feeder can be completely neglected. In fact, it is assumed that such an antenna is fed by a symmetrical (balanced) transmission line, and that the signal source U_{SC} is also symmetrical with respect to the ground. In other words, the source U_{SC} is replaced by two sources each of half the voltage of the original one, connected in series with the common node grounded (**Figure 1B**). Moreover, it is assumed that the symmetrical feed line runs perpendicularly to the antenna all the way down to the signal source and, thanks to the symmetry, it does not pick up any RF energy radiated by the dipole.

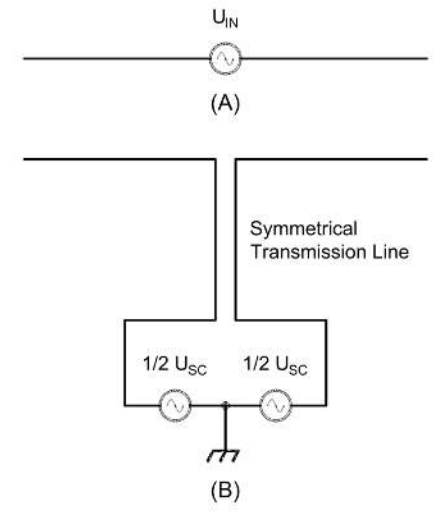

Figure 1 — A common way of modeling a half-wave dipole (A), and the circuit that is actually assumed in this way (B).

Modeling an Antenna with a Coax Feeder

In the majority of implementations of ham antennas, a 50 Ω coaxial cable rather than a symmetrical line is used for antenna feeding. The actual circuit is shown in **Figure 2A**. Let's ignore for the time being any matching networks or baluns or common-mode chokes at the feed point. As you can see, the signal source and the transmission line are no longer symmetrical. In such a network, some imbalance of the transmission line currents must happen. There are two reasons for this. The signal source is no longer split in two equal sources with a grounded common point, but is now a single source with one terminal grounded. The two conductors of the transmission line have different electromagnetic coupling to ground and to the dipole legs what becomes important when the feeder is not exactly vertical. The imbalance of the transmission line current is called the CMC, and is almost

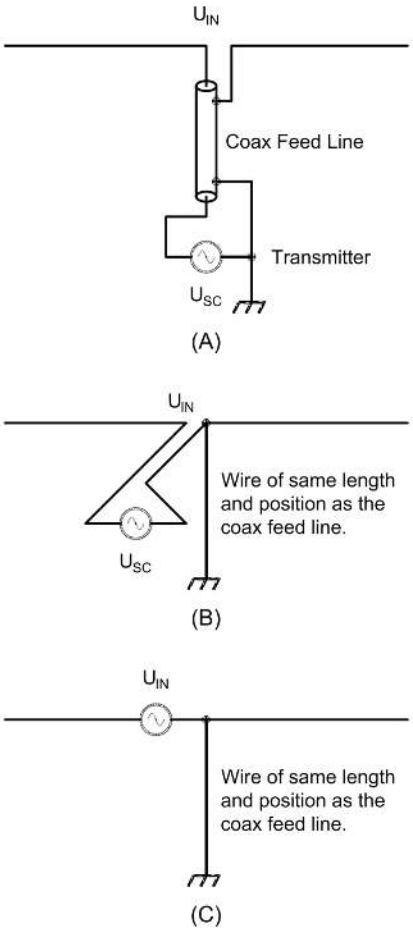

Figure 2 — The circuit of the coax-fed antenna (A) can be modeled as in (B) or (C).

never desirable because it makes the feeder radiate RF energy. It would be useful to simulate how much CMC we can expect in the shield of coax if we connect it to the feed point of our antenna. Knowing that, we could decide if such a value is acceptable and if not, introduce some modification to the antenna or to the feeder to reduce this current.

Current antenna simulators available to amateurs do not offer the "coax cable" object that could be added to the antenna model like a wire or an *RLC* trap. However, as Roy Lewallen, W7EL, explained it in his user manual to the *EZNEC* program, we can use an idealized transmission line along with a wire for the purpose as presented in **Figure 2B**. In computer simulations, the idealized transmission line does not pick up any electromagnetic radiation from the antenna elements nor does it interact with the ground. It only transfers the source power to the antenna feed point and transforms antenna impedance in accordance with its parameters (length and characteristic impedance). That's what is available in *4nec2*. *EZNEC* as well as *AutoEZ* in combination with *EZNEC* do allow the designer to additionally specify coax loss. Nevertheless, such a transmission line is still an idealized object and it does not matter where you put it in the antenna model. Even if you place it at an angle as in **Figure 2 B**, it will not pick up any radiation from the antenna and will not impact its radiation pattern.

In order to simulate the coax feeder interaction with the antenna and the ground, an additional wire is needed in the model. It should be placed in the same position as the actual feeder. For the most accurate results, this additional wire should be made of the same material and have the same diameter as the coax shield and have the same insulation as the coax cable. This wire should be grounded in the place where the actual feeder touches the ground. If the feeder does not touch the ground in the actual application, you should extend the wire emulating coax in the model with an additional wire connected between the end of the coax and ground. This will emulate the grounding wire of your station.

It is possible to simplify the circuit to the form shown in **Figure 2C**. Knowing the coax parameters and the SWR at the antenna feed point, you can calculate how much transmitter power will be lost in the coax before it reaches the feed point. To do that, you can use *TLDetails* program by Dan Maguire, AC6LA, or a similar calculator. In the circuit shown in **Figure 2C** the signal source is placed directly at the feed point, but the transmitter power is reduced by the loss in the coax. In such a model the current that flows in the wire emulating the feeder is equal to the CMC or, in other words, to the difference between the two currents that flow in the center wire and on the shield of the real coax.

When doing routine antenna simulations with a single signal source, you normally do not care how much power the signal source delivers. The input power of the source does not influence the antenna radiation pattern, SWR or feed point impedance. But when you want to assess the currents in the antenna wires or the CMC in the feeder during transmission, you should set the expected value of input power. The antenna input voltage U_{IN} shown in **Figures 1 and 2** depends on the antenna input impedance and the RF power that is delivered to the feed point. When simulating an antenna, you do not specify U_{IN} but rather the power input. When you run a simulation, the software calculates the antenna impedance and then, knowing the input power, it calculates the input voltage U_{IN}. Examining simulation results, you can find out the input voltage calculated by the program.

When simulating an antenna with a coax feeder, except for the normal antenna parameters, you will also be interested in the current flowing in the wire emulating the coax shield. Simulators like *4nec2* or *AutoEZ*+ *EZNEC* can deliver information on the current flowing in every segment of this wire. Generally, the CMC will have different values in different segments of the feeder. You need to find the maximum value of the current along the whole length of the feeder and compare it with the limit you want to put on the CMC. More on this limit setting later.

To analyze the CMC mechanism in more detail, it is convenient to think of the antenna as a common-mode voltage source U_{CM} connected in series with the antenna common-mode impedance Z_{ACM}. In many antenna installations, there are chokes or current baluns inserted between the antenna and the feeder. Let's assign symbol Z_{CH} to the choke/balun common-mode impedance. Z_{FDR} symbol will be assigned to the impedance of the feeder (coax shield) as seen from the choke perspective. Z_{GND} will be the impedance representing losses in the ground. The circuit for calculating the maximum value of the CMC is in **Figure 3**.

U_{CM}, Z_{ACM} depend on the antenna type and U_{CM} additionally depends on U_{IN}. Z_{CH}

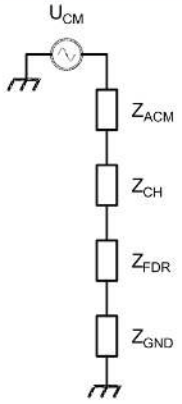

Figure 3 — Equivalent circuit of the antenna and feeder for calculating maximum value of the CMC.

depends on the choke/balun design. If the antenna is fed without a choke or with a voltage balun, Z_{CH} equals zero.

Impedance of the feeder Z_{FDR}, as seen from the choke perspective, changes from nearly zero for the lengths equal to the even multiples of λ/4 (λ/2, λ, 3λ/2, …) to very high impedance for the lengths equal to odd multiples of λ/4 (λ/4, 3λ/4, 5λ/4, …). For the antennas with low input impedance, the most unfortunate feeder lengths are those close to the even multiples of λ/4. If no choke is used, a very high CMC will flow through such a feeder.

Z_{GND} is usually considered to be a pure resistance. In normal cases, its value is in the order of tens of ohms and it has marginal effect on the CMC reduction and can be neglected.

Electrically Balanced Antennas

Let's examine (**Table 1**) U_{CM} and Z_{ACM} for a few symmetrical antennas: half-wave dipole, intermittent half-wave quad loop (monoband Cobweb) and a folded dipole with three different wire spacings *d*. All of them were designed for the 75/80 m band (3.75 MHz center frequency) and placed 40.86 m (λ/2) above ground level. The input power was set to 100 W. The wire simulating the coax was positioned vertically from one terminal of the source to the ground. The simulation results are shown in **Table 1**.

For the half-wave dipole and the Cobweb, the common-mode voltage U_{CM} equals half the input voltage U_{IN}. However, this is not a rule as the results of the folded dipole show. For that antenna type, U_{CM} is closer to 2/3 of U_{IN}. All of the simulated antennas had quite small common-mode impedance, not helping much in reducing CMC.

Table 1 – Input and common-mode parameters for different symmetrical antennas.

Antenna	U_{IN}, V	Z_{IN}, Ω	U_{CM}, V	Z_{ACM}, Ω
Half-wave dipole	82.1	67.5 + *j*0	40	23 + *j*0
Cobweb	35.2	12.2 + *j*1.8	17	23 – *j*11
Folded dipole, d = 0.2 m	164	270 + *j*0	106	66 + *j*0
Folded dipole, d = 0.5 m	164	269 + *j*0	104	80 + *j*0
Folded dipole, d = 1 m	163	267 + *j*0	105	95 + *j*0

Based on the above simulations, we can say that antennas having larger input impedance will create greater common-mode voltage and will require higher value of Z_{CH} and/or Z_{FDR} to keep the CMC below the threshold.

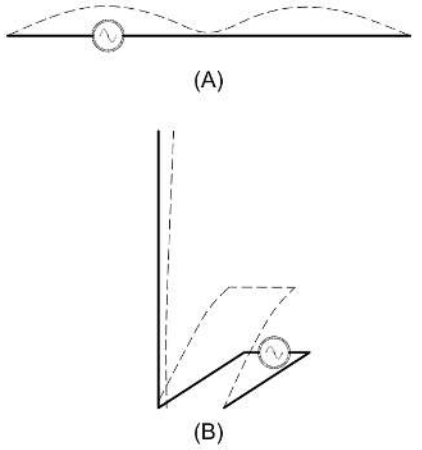

Figure 4 — Asymmetrical antennas can be electrically balanced if they have their feed points located in current maximum spots. The dotted lines show current magnitudes.

When the antenna is not used at its resonant frequency, its input impedance changes, it usually grows. As a result, the input voltage is greater and also the common-mode voltage is greater. For example the half-wave dipole shown in **Table 1**, when operated at 3.5 MHz, will have the following parameters: U_{IN} = 168 V, Z_{IN} = 62 – *j*120 Ω, U_{CM} = 82 V and Z_{ACM} = 48 – *j*4 Ω. As you can see, the common-mode voltage U_{CM} has doubled.

Another important observation is that the antenna does not need to be physically symmetrical to behave like an electrically balanced antenna, that is, to have a small value of U_{CM}. An example of such antenna can be a modified dipole having one leg λ/4 long and the other 3λ/4 long, see **Figure 4A**. Another example is in **Figure 4B**. This is the end-fed Zepp with a vertical half-wave radiator and horizontal λ/4 stub (only a fragment of the antenna is shown for better clarity). Antennas like that have their feed points located at the current maxima. In such a case, the antenna input impedance is small and current distribution around the feed point is symmetrical. Thanks to that, the antenna is electrically balanced from the perspective of the signal source and its common-mode voltage U_{CM} is small — less

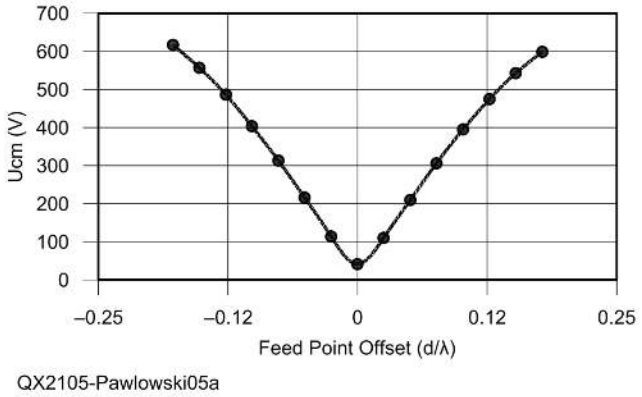

Figure 5 — Antenna common-mode voltage U_{CM} (for 100 W) and common-mode impedance Z_{ACM} for the off-center-fed half wave dipole.

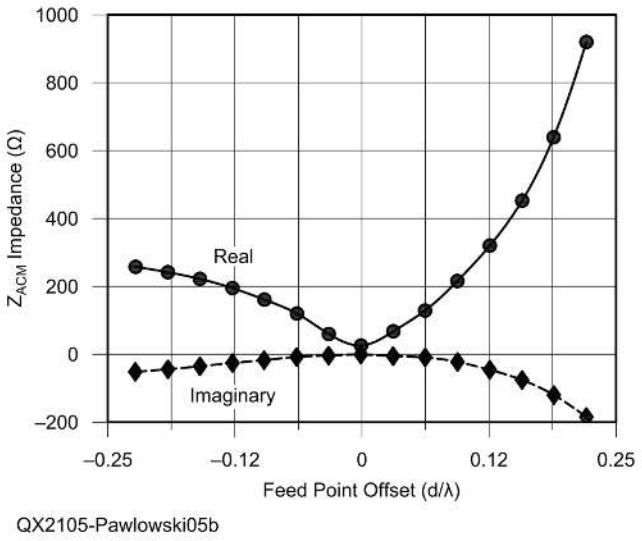

Table 2– Equivalent RLC circuit components calculated for a choke wound on a 2.4" O.D. ferrite toroid core of #43 material. RLC values are valid for 1 to 55 MHz range. Calculation based on the data published in [1]. The resonance frequency is provided for orientation only.

No. of turns	R_C, kΩ	L_C, µH	C_C, pF	F_0, MHz
6	2.3	32	1.8	21
7	2.8	46	1.9	17
8	3.6	60	2	14.5
9	4.4	80	2.1	12.5
10	5.2	95	2.3	11
11	6	120	2.4	9.5
12	7	140	2.5	8.5
13	8	170	2.5	7.7
14	9	200	2.7	7

than 100 V for 100 W power input for both exemplary antennas.

If the antenna is physically symmetrical, it is easy to say how to route the feeder so that it picks up minimum radiated RF energy by the antenna. It may not be so obvious if the antenna is electrically balanced but not physically symmetrical as those in **Figure 4**. Then, a simulation can help find the best way of routing the feeder.

Unbalanced Antennas

The off-center-fed dipole (OCFD) is definitely an unbalanced antenna. **Figures 5A and 5B** show plots of its common-mode voltage and common-mode impedance as a function of the feed point offset. The more the feed point is moved off the antenna center, the greater the common-mode voltage is generated. The voltage rise is steep. The most popular version of the OCFD has a leg length ratio of 1:2. The U_{CM} for such a version is about 330 V compare to 41 V for a center-fed dipole. The difference is striking. It is evident that achieving small CMC in the feeder of an unbalanced antenna is more difficult. A very high impedance common-mode choke or even a number of such chokes is needed.

Common-mode Chokes

The two most popular common-mode chokes are the air-wound ones — coiled with a lengths of coax without any magnetic core — and the ones wound on the toroid ferrite core(s). There are also chokes made of ferrite beads or multi-aperture ferrite cores but they are less popular in ham antenna designs.

The air-wound chokes have very sharp parallel resonance curve and because of that their performance are hard to control. Their reactance depends on the dimensions, winding style and coupling to nearby conductors. Even relatively small change of any of these factors will shift the resonance from the desired frequency where the chokes have maximum impedance. When they are operated below or above resonance, their impedance and thus their impact on the CMC is greatly reduced.

Let's focus on the chokes wound on the ferrite cores. It has been established that their common-mode impedance can be approximated by a parallel *RLC* resonance circuit. Depending on the material, they can have either one or two resonances: circuit resonance or a dimensional resonance. The nickel zinc ferrites (materials #43, #61) have only a circuit resonance but the manganese zinc ferrites (material #31) have both. Their equivalent circuit consists of either a single parallel *RLC* circuit (**Figure 6A**) or two parallel *RLC* circuits connected in series (**Figure 6B**).

Let's consider the simpler circuit shown in **Figure 6A**. The highest impedance occurs at circuit resonant frequency and is equal to R_C. At the resonant frequency F_0 the choke impedance Z_{CH0} is equal to its resistance:

$$Z_{CH0} = R_C \quad \text{for } F = F_0 \ .$$

For frequency F_1, which is lower than the resonant frequency F_0, the choke Z_{CH1} impedance has an inductive reactance component:

$$Z_{CH1} = R_1 + jX_1 \quad \text{for } F = F_1 < F_0 \ .$$

Note that the resistive component of this impedance is smaller than R_C:

$$R_1 < R_C$$

and even the magnitude of the total impedance is smaller than the R_C:

$$|Z_{CH1}| = \sqrt{R_1^2 + X_1^2} < R_C \ .$$

We have a similar situation when frequency F_2 is higher than the resonant frequency F_0. The choke impedance Z_{CH2} now has a capacitive reactance component:

$$Z_{CH2} = R_2 - jX_2 \quad \text{for } F = F_2 > F_0 \ .$$

The resistive component of the impedance is again smaller than R_C:

$$R_2 < R_C$$

and the magnitude of the total impedance is also smaller than R_C:

$$|Z_{CH2}| = \sqrt{R_2^2 + X_2^2} < R_C \ .$$

You can see all these relationships in the plot shown in **Figure 7**. Plots of this kind have been published for different ferrite core chokes by Jim Brown, K9YC **[1]**, and Ian White, GM3SEK **[2]**. With such plots, you can find the *R* and *X* components for a frequency of interest. *R* is given explicitly on the plot and *X* can be calculated from:

$$X = \pm\sqrt{|Z|^2 - R^2}$$

where *X* is positive for the frequencies smaller than the resonant frequency and negative for the frequencies greater than the resonant frequency.

Using *R* and *X* is not very convenient when modeling antennas because they are valid only for a single frequency. If you want to change frequency (for example to check the band edges) you need to edit the model file and substitute *R* and *X* values with the new ones.

If you knew the values of the equivalent circuit components: R_C, L_C and C_C (and for some materials also R_D, L_D and C_D), you could use them directly in the model as a parallel *RLC* circuit (or two such circuits in series) and have the correct choke impedance for any frequency. Because the *RLC* component values of the equivalent circuits are rarely available, I have calculated them for a number of chokes for which the $|Z_{CH}|$ *vs.* *F* plots were available. The results are gathered in **Tables 2 through 5**.

Two Ways of Exciting CMCs

The CMC can be excited by conduction and by radiation. When we consider the common-mode voltage U_{CM} and a series of impedances as shown in **Figure 3**, we deal only with the current excited by conduction. But the coax shield can pick up electromagnetic radiation from the antenna. This generates a CMC and the feeder becomes an additional unwanted antenna

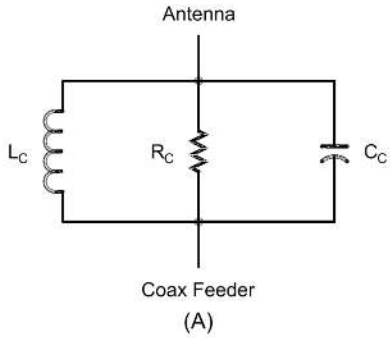

QX2105-Pawlowski06a

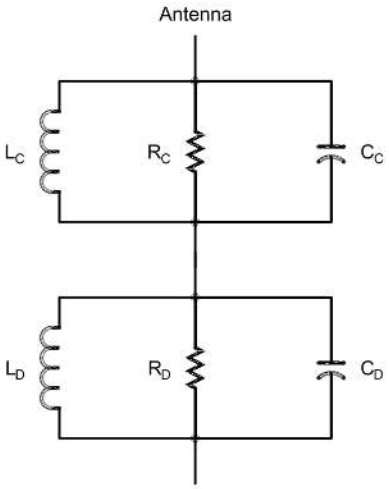

QX2105-Pawlowski06b

Figure 6 — Equivalent circuits of common-mode chokes – single resonance circuit (A), and double resonance circuit (B).

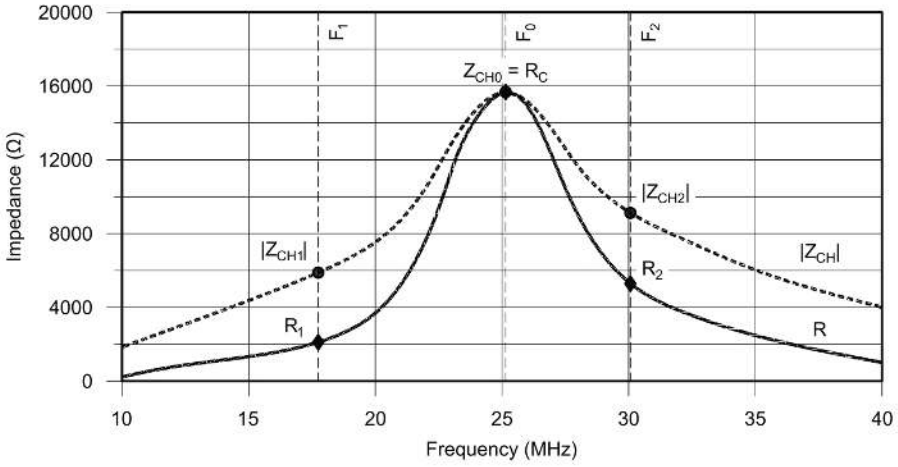

QX2105-Pawlowski07

Figure 7 — Common-mode impedance magnitude $|Z_{CH}|$ and its resistive component R versus frequency F for an example common-mode choke.

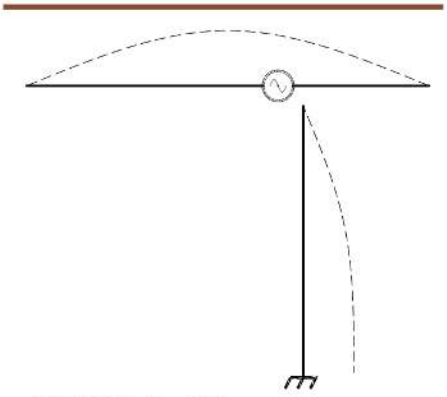

QX2105-Pawlowski08

Figure 8 — The CMC excited by radiation in OCFD. The dashed lines show the current magnitude. Note that the λ/4 long feeder is disconnected from the antenna to simulate a choke of infinite impedance.

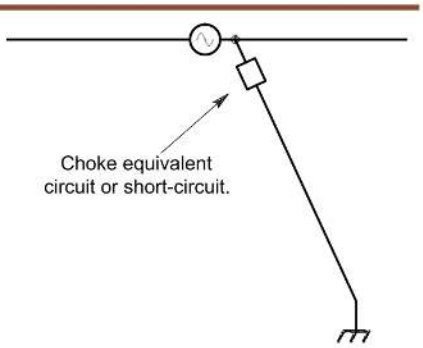

Figure 9 — Example #2: the horizontal center-fed half-wave dipole with the feeder run askew.

element. Exciting currents by radiation always happens if the coax is not placed such that it does not pick up any radiation from the antenna, for example, if the feeder is not perpendicular to a center-fed dipole.

Let's consider an OCFD with a choke of infinite impedance installed at the feed point (**Figure 8**). The wire emulating the coax is disconnected from the antenna to simulate a choke of infinite impedance. Obviously, there is no CMC due to U_{CM} because the circuit is broken. Yet, if the coax length is about λ/4 long, a large current will be induced on its shield due to radiation from the antenna. The same situation will happen if the coax of a center-fed dipole is not routed vertically down but is askew. Even with the very best choke, the CMC will be excited in the feeder.

The good news is the antenna simulators calculate the CMC excited in both ways at the same time. No need to worry that the

Table 3– Equivalent RLC circuit components calculated for a choke wound on a 2.4" O.D. ferrite toroid core of #61 material. RLC values are valid for 1 to 55 MHz range. Calculation based on the data published in [1]. The resonance frequency is provided for orientation only.

No. of turns	R_C, kΩ	L_C, μH	C_C, pF	F_0, MHz
6	4.1	8.6	2.6	33.5
7	5.2	10.5	2.9	29.0
8	7.8	13.2	2.9	25.5
9	17.0	16	3.0	23.0
10	17.5	20	3.0	20.5
11	18	24	3.1	18.5
12	20	28	3.1	17.0
13	22	32.5	3.1	16.0
14	18	38	3.2	14.5

simulation results will be in disagreement with the real world values. Nevertheless, it is good to understand these two ways of exciting CMCs because the simulation results might otherwise be confusing.

Impact of Feeder Length

The feeder impedance Z_{FDR} influences the CMC excited by conduction. The impedance depends on coax length. If the feeder is about λ/4 long, it can be represented by a parallel *RLC* circuit with large *R* component (> 3 kΩ). However, if the feeder is about λ/2 long it is equivalent to a series *RLC* circuit with small *R* value (< 50 Ω).

The CMC excited by radiation depends on coax length. **Table 6** can help you predict what coax lengths are most likely to cause the CMC problem due to conduction and due to radiation. Note that the coax length is measured from the feed point (or the choke if used) to the point when we can consider it grounded. It is usually assumed that this is the point where it touches the ground for the first time.

The prediction depends on antenna feed point impedance. Most of the currently used antennas have a low feed point impedance but, for example, the extended Zepp has high feed point impedance.

Systems with low feed point impedance antennas benefit from the common-mode choke only if the coax length is close to the even multiples of λ/4 (λ/2, λ, 3λ/2, …). But the choke is not effective and can even increase the CMC when the coax length is close to odd multitudes of λ/4, that is, (λ/4, 3λ/4, 5λ/4, …) unless the antenna is symmetrical and feeder is run in such a way to not pick up any radiation from the antenna.

An interesting article by Rich Quick, W4RQ, and Kai Siwiak, KE4PT **[4]**, shows how CMC varies depending on the length of a coax feeder connected to a dipole.

Table 4 – Equivalent RLC circuit components calculated for a choke wound on a 2.4" O.D. ferrite toroid core of #31 material. RLC values are valid for 1 to 55 MHz range. Calculation based on the data published in [1].

No. of turns	R_D, kΩ	L_D, μH	C_D, pF	R_C, kΩ	L_C, μH	C_C, pF
6	0.65	110	55	1.95	15.5	2.6
7	0.95	170	28	2.4	19	2.8
8	1.2	200	25	2.7	26	2.9
9	1.55	240	23	3.1	36	3
10	2	290	17	3.4	40	3.5
11	2.5	350	12	3.2	44	3.9
12	3	440	10	3.1	55	4.4
13	3.55	520	8.5	3.0	67	5
14	4.4	620	6.7	2.75	59	6.7

Table 5 – Equivalent RLC circuit components calculated for the chokes described in [2] and wound on the oval ferrite cores of #43 material. RLC values are valid for 1 to 30 MHz range. The resonance frequency provided for orientation only.

Choke type	R_C, kΩ	L_C, μH	C_C, pF	F_0, MHz
Low Bands	6.2	280	14	2.5
Mid Bands	4.7	95	3.5	8.7
High Bands	2.3	23	2.2	22.4

Table 6 – Types of the CMC excitation (c - by conduction, r - by radiation) depending on the feeder length in wave lengths, antenna feed point (FP) impedance and presence or absence of common-mode choke.

Antenna system	λ/4	λ/2	3λ/4	λ	5λ/4	3 λ/2
Low FP impedance, no choke	–	c	–	c	–	c
Low FP impedance, high Z choke	r	–	r	–	r	–
High FP impedance, no choke	c & r	–	c & r	–	c & r	–
High FP impedance, high Z choke	c & r	–	c & r	–	c & r	–

Antenna System Examples

When simulating the antenna-choke-feeder system, you should use the circuit shown in **Figure 2C or 2B**. The feeder geometry should be the same as the your coax geometry. If the coax is not routed vertically but at some angle, model the wire emulating coax shield at the same angle. If the choke is used at the feed point, add a parallel *RLC* circuit to the first segment of the coax emulating wire. If you need two *RLC* circuits, you can add the second one to the second segment of the wire or again to the first segment of the wire. Contemporary antenna simulators will allow you to add two parallel *RLC* circuits connected in series to the same wire segment (**www.arrl.org/QEXfiles**).

Before we move on, we need to establish the limits we can tolerate for the maximum CMC and maximum power dissipated in the choke (if used). When setting the first limit, I compare the CMC to the current flowing in a center fed dipole with 4 watts of RF power applied to it. That is the power level we have in our hand-held transceivers, and it corresponds to 240 mA of the CMC. This may seem like a large current if you remember that for a center-fed dipole fed with 100 W power, the current near the feed point is 1.2 A. Everything is okay, since if the current is reduced by a factor of 5, the power is reduced a factor of 25.

I usually accept 10 W as the maximum power that can be dissipated in the common-mode choke when the system is fed with 100 W at the feed point. This may again look high but losing 10% of power weakens your signal by just 0.5 dB.

Example #1

Let's analyze a few antenna systems. The first one is *the horizontal center-fed half-wave dipole with vertical feeder*. This is a symmetrical antenna with the feeder located in a manner to pick up as little radiation from the antenna as possible.

My model looks like **Figure 2C**. The most problematic feeder lengths are even multiples of a λ/4. I used the antenna simulator to find out what is the feeder length range near λ/2 that would result in a CMC greater than 240 mA when 100 W is applied to the feed point. The simulations were run for a dipole tuned to 3.75 MHz. For this frequency, the feeder length range causing problems was 0.46λ to 0.56λ. Such range of 'prohibited' coax lengths seemed to be relatively narrow, but that was true only for the single frequency 3.75

MHz. Simulations for the same antenna but frequencies between 3.5 MHz and 4 MHz revealed that troubles could be expected for the feeder lengths between 0.39λ and 0.65λ. The worst case CMC reached 1.8 to 2.3 A depending on frequency. These calculations proved that you should simulate the CMC not only for the frequency in the center of the band but also at the band edges.

The next step was simulating the same antenna with a common-mode choke added at the feed point. The system was simulated with the following chokes:

- choke A: 2.4" ferrite toroid core, material #43, 14 turns.
- choke B: 2.4" ferrite toroid core, material #31, 14 turns.
- choke C: the "Low Bands" choke wound on three oval cores, material #43, 5 turns.

Every choke reduced the CMC down to 15 to 25 mA when the feeder length was close to λ/2. This is a dramatic improvement over the system without a choke.

The feeder lengths close to λ/2 were no longer the worst cases. Note that modeling a center-fed dipole in the way shown in **Figure 2C** introduced a small imbalance. The signal source was in one antenna leg only. This caused a small asymmetry in the current distribution over the antenna wires that in turn excited some CMC. **Table 7** shows that if a choke was added, the worst case current happened for the feeder lengths near λ/4. There are some differences in the worst-case lengths depending on the choke type because their impedances are not equal and differ not only in resistive components but also in reactive (capacitive or inductive) components at a given frequency. Fortunately, the worst case currents for all the systems with chokes were below the limit of 240 mA, also for the feeder lengths near λ/4. Power dissipated in the chokes was negligible so we achieved a design good for any coax lengths. But remember about the initial condition: the feeder goes perfectly vertical and touches ground below the center of the dipole.

Example #2

The next example is the *horizontal center-fed half-wave dipole with fixed length feeder run askew* (**Figure 9**). The antenna was 2 times 19.64 m long, 16 m above ground and its feeder consisted of 16.8 m long tilted section, and 2.5 m long vertical section. So, the total feeder length was close to λ/4.

When simulated at 3.75 MHz with choke B placed at the feed point, the CMC in the feeder exceeded 530 mA. At the same time, the power dissipated in the choke exceeded 13 W. So, both limits, 240 mA and 10 W, were exceeded.

However, when the choke was removed and the feeder was connected directly to the right arm of the antenna, the CMC dropped to 91 mA and, of course, there was no power loss in the choke because it had been removed. It demonstrates that sometimes it is much wiser not to use a common-mode choke.

Example #3

The third example is the antenna known for its high common-mode voltage U_{CM} – the C—pole. The design I started with was proposed by B. V. Cake, KF2YN **[3]**. I modeled and simulated the 20 m band version repeating the antenna dimensions after the author.

I selected the best choke for this frequency which was the 14-turns choke wound on material #61 (see **Table 3**). The calculated maximum CMC was only 35 mA at 14.175 MHz. That's very good but unfortunately the power dissipated in the choke was no less but 17.5 W. It often happens with the unbalanced antennas using chokes that the power dissipation is the limiting factor not the CMC. One way to overcome this problem is to add yet another identical choke in series with the first one. Five watts will be dissipated in every choke, so 10 watts in total. The CMC will drop to 17 mA.

The other possible way to make this antenna work efficiently is to move the feed point to the current maximum spot as shown in **Figure 10 (B)** and connect the feeder without any choke. The CMC will

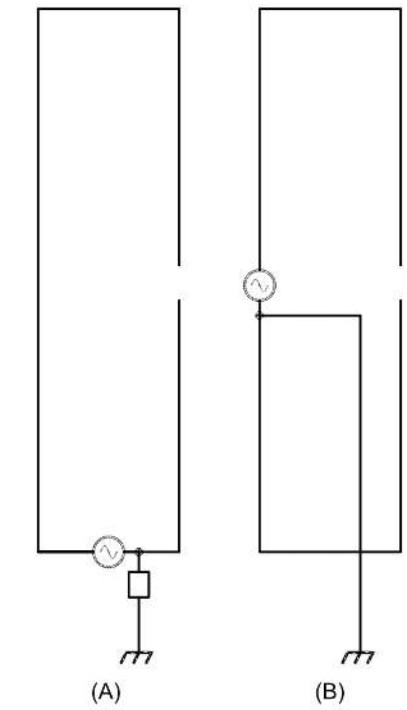

Figure 10 — Example #3: the C-pole as originally designed (A), and with the feed point moved and choke omitted (B).

Table 7 – Worst case CMCs excited in a 80/75 m band center-fed dipole for different chokes.

CMC type	*Freq., MHz*	*Worst case CMC, mA*	*Power dissipated in choke, W*	*Worst case feeder length, m*	*Worst case feeder length, λ*
No choke	3.5	2200	n/a	44.4	0.52
No choke	3.75	1800	n/a	40.8	0.51
No choke	4.0	2300	n/a	37.8	0.50
A	3.5	97	0.5	22.4	0.26
A	3.75	75	0.2	20.6	0.26
A	4.0	124	0.6	19.2	0.26
B	3.5	71	0.1	21.0	0.25
B	3.75	62	0.01	19.4	0.24
B	4.0	114	0.3	18.0	0.24
C	3.5	87	0.3	19.8	0.23
C	3.75	85	0.3	18.2	0.23
C	4.0	175	1.4	16.8	0.22

be then 206 mA and of course there will be no power dissipated in the choke. The feed point impedance will change from about 50 Ω to about 30 Ω, so you will have to decide whether to add a suitable un-un (not introducing common-mode impedance) or to accept some mismatch. I would personally go for the second option.

Conclusion

The battle with the CMC in the coax feed line does not end once you add a common-mode choke at the antenna feed point. As a matter of fact, in some cases, the presence of the choke may worsen the situation. In badly designed antenna systems, it may happen that too much power is dissipated in the choke that can lead to a failure and is a waste of the transmitter power. Fortunately, thanks to the antenna simulation software, we can first simulate various cases and avoid nasty surprises. This is a much better approach than trial and error method when the real antenna is already built and installed. I hope that this article will encourage my fellow antenna designers to simulate antennas along with the chokes and feeders. It is not very complex!

Jacek Pawlowski, SP3L, is an electronics engineer with a MSc degree. He started his professional career as an electronic designer, in testing and measurements. After about 15 years as a circuit and PCB designer, he switched to a management career path. He has been an R&D project and R&D department manager in several companies since then. Jacek caught his radio bug when he was still in a primary school in the early 1970s. In the years 1978 to 1999 he was active as SP3LFV. After that he suspended the hobby for 15 years. In 2014, he became active again under the new call sign, SP3L. Jacek maintains a web page, **https://sites.google.com/view/sp3l-hf-antennas/home-page**, *of his antenna designs.*

Literature

[1] J. Brown, K9YC, "A Ham's Guide to RFI, Ferrites, Baluns, and Audio Interfacing," Revision 7 Jan. 2019; **k9yc.com/RFI-Ham.pdf**.

[2] I. White, GM3SEK, "Cost-effective ferrite chokes and baluns"; **www.ifwtech.co.uk/g3sek/in-prac/inpr1005_ext_v2.pdf**.

[3] B. V. Cake, KF2YN, "The 'C Pole'— A Ground Independent Vertical Antenna," *QST* Apr. 2004; **https://noji.com/hamradio/pdf-ppt/C-Pole-Antenna.pdf**.

[4] R. Quick, W4RQ, and K. Siwiak, KE4PT, "Does Your Antenna Need a Choke or a Balun?," *QST*, Mar. 2017, pp. 30-33.

Announcement

Cross of Merit of the Federal Republic of Germany Awarded to Professor Ulrich L. Rohde, N1UL

Following the nomination by Dr. Markus Söder, President of the German State of Bavaria and Member of the Bavarian Parliament, the Federal President has awarded Professor Ulrich L. Rohde the *Cross of Merit of the Federal Republic of Germany*. The Award recognizes Dr. Rohde's significant contribution to Germany's technological advances, prosperity and security work as a scientist, university lecturer, developer and entrepreneur in the fields of radio frequency and microwave technology.

The Order of Merit of the Federal Republic of Germany, established in 1951 by then Federal President Theodor Heuss, is the highest tribute the Federal Republic of Germany can pay to individuals for services to the nation. The Order comprises nine classes in the groups Medal of Merit, Order of Merit, Great Cross of Merit and Grand Cross, and may be awarded to Germans and foreign nationals alike.

QEX joins in congratulating Professor Ulrich L. Rohde, N1UL, a frequent *QEX* author, on achieving such a high honor.

Feedback

A Four-Band Two-Element W7SX (Zavrel) Array (Mar./Apr. 2021)

Dear Editor,

A description of a mono-band extended-element beam was published by:
R. C. Fenwick, K5RR, R. C. Fenwick Jr., N5BXB, and B. Schroeder, "The Extended-Element Beam," *QST*, Dec., 1983. — *Best regards, Bob Zavrel, W7SX.*

Tony Brock-Fisher, K1KP
15 Webster St., Andover, MA 01810; **k1kp@arrl.net**

Fixture and Method for Measuring Q of Inductors Using a VNA or Spectrum Analyzer

Use a capacitor in parallel with the inductor under test to measure the Q from transmission loss.

During the course of several projects I needed to measure the Q of an iron powder core toroidal inductor. For high values of Q, this is not a simple or easy measurement to make. I had a couple of VNAs and a spectrum analyzer (SA) available to me as possible measurement tools, but I needed to determine the best way to measure Q without introducing unacceptable measurement errors. This note describes a method of measuring inductor Q with reasonable accuracy using either an inexpensive VNA (or antenna analyzer) or an SA.

One of my VNAs is the recently introduced nanoVNA, which is an inexpensive two-port VNA that provides excellent capabilities. It can be calibrated using the customary short, open, 50 Ω load standards. As a two-port VNA, it can be calibrated to make transmission loss measurements. An inductor can be connected directly to the CH0 input and the nanoVNA. Use the *NanoVNASaver* software **[1]** to directly report the inductance and Q at a chosen frequency. However, for reasonably high values of Q, the accuracy of the Q value reported by the nanoVNA is questionable and highly dependent on the calibration in effect.

The measurement of Q requires knowing the inductance and series resistance of the unknown inductor, then,

$$Q = \frac{2\pi f L}{R_S}$$

For high Q inductors, R_S is typically very low, and attempting to measure a small resistance in series with an inductor becomes difficult and error prone. It's similar to measuring very small resistances at dc with an ohmmeter where a different approach, such as a 4-wire measurement technique, is required to get accurate results. Clearly a different approach is needed.

Circuits for Measuring Q

I searched the web and found another technique **[2]**, wherein the unknown inductor to be measured is connected in series with a known capacitor to form a series resonant circuit. This series *LC* circuit is then connected in series with a fixed 50 Ω resistor, and the VNA is used to measure the resistance at resonance, see **Figure 1**.

The Q of the capacitor is assumed to be much larger than the Q of the inductor, as is usually the case **[3]**, so the resultant measured resistance is assumed to be the sum of R_S of the inductor with the fixed resistor. The typical VNA (or antenna analyzer) is presumed to be most accurate near 50 Ω, so small deltas can be measured. I tried this approach with the nanoVNA, but found that the measurement was highly dependent on the calibration, and often gave negative values for R_S. Therefore the technique was not useful when using the nanoVNA.

The combination of the unknown inductor with a capacitor to form a parallel resonant circuit gives a circuit that can be measured and the response curve can be analyzed to determine the Q of the parallel circuit. Again, the Q will be dominated by the Q of the inductor, which is typically lower than the Q of the capacitor by a factor of 5 or more, so the Q of the circuit largely

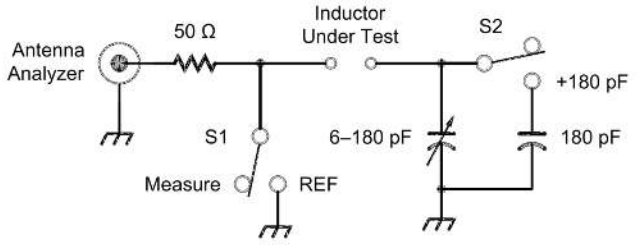

Figure 1 — Inductor Q measurement circuit by Phil Salas, AD5X.

represents the Q of the inductor.

A parallel resonant circuit can be analyzed using a VNA or SA in the two-port mode. The parallel resonant circuit is inserted between the output of CH0 of a nanoVNA (or the tracking generator output of the SA) and the CH1 input of the nanoVNA (or the signal input of an SA). In this configuration, the parallel *LC* circuit is driven from a 50 Ω source and terminated by a 50 Ω load impedance of the CH1 or SA input, see **Figure 2**.

Simulating the Circuit

This configuration was simulated in *LTspice*. The ac response of the circuit was measured and the Q determined from the ac response. The inductor Q was adjusted over a range of interest by entering nonzero values for the series resistance of the inductor in the simulation. Reasonable agreement between the measured and directly computed values of Q was found. To investigate the effect of loading by the source and load impedance of the measurement instrument, the 50 Ω termination resistances for the source and load were changed to 100 Ω, for a case with no series resistance in either the inductor or the capacitor (theoretically an infinite Q). No change was seen in the measured Q as the termination values were changed. The measured Q of 1605 was less than infinite due to finite sampling of the frequency response curve, which in this example was 200 points over 2 MHz. If the sampling was increased to 200 points over 5 MHz the measured Q increased to 6417.

Additionally, the assumption that the Q of the capacitor was not a large error in measuring the Q of the inductor was investigated. Two analyses were run in *LTspice*. The first was with 1 Ω series resistance for the inductor and 0 Ω series resistance of the capacitor. This gave a Q of 181. Then the series resistance of the capacitor was set to 0.1 Ω, which represents a Q of 1020. The measured Q of the inductor came down to 160. This was not a large discrepancy. Furthermore the Q of the capacitor acts to underestimate the Q of the inductor, which would be a conservative error for most applications — higher Q is nearly always better.

This measurement technique is best suited for inductors using iron-powder cores where the coil Q is around 200. For air core inductors, the inductor Q can be much higher **[4]**, and in these cases the Q of the capacitor can have a greater effect on the accuracy of the measurement.

The capacitor value used can be adjusted to change the resonant frequency. The frequency of resonance defines the frequency where the Q of the inductor is measured. Often it is desired to measure the Q at a specific frequency, or at multiple frequencies. Therefore it is useful to use a variable capacitor.

Test Fixture

A test fixture specifically for measuring the Q of inductors was fabricated, see **Figure 3**. I used a dual-section air variable capacitor with about 380 pF per section. For small inductors and low frequencies, the second section of the capacitor can be added to the circuit with a short clip lead, or a toggle switch could be added. Because the frame of the capacitor is one terminal but is not connected to ground, I mounted the variable capacitor to a piece of copper clad PCB material using nylon screws and washers. SMA connectors were added to use the fixture with the nanoVNA, but BNC connectors could be used with another VNA or SA. Alligator clips were included to connect to the inductor to be tested.

To use the fixture, connect it to the VNA in two-port mode. The measurement to be made on the VNA is the transmission loss measurement between port 1 and port 2 (CH0 and CH1). With a parallel resonant circuit, the transmission loss will be low above and below the resonant frequency, and will be much greater at the resonant frequency. To measure Q, two or three points must be measured on the curve. The resonant frequency and the upper and lower frequencies where the transmission loss is 3 dB lower than the peak must be measured, see **Figure 4**. The center (resonant) frequency can be directly measured as the frequency of maximum transmission loss, or it can be assumed that the response curve is symmetrical and the resonant frequency can be interpolated as the average of the two other points. The Q of the circuit, which approximates the Q of the inductor is,

$$Q = \frac{F_{res}}{F^{+}_{3dB} - F^{-}_{3dB}}.$$

If your VNA can export the transmission loss data, you can import the data into an Excel spreadsheet and automatically compute the Q. If you're using an older SA or VNA, then you'll have to make the measurements and computations manually. An Excel spreadsheet for computing Q from such data is available at **www.arrl.org/QEXfiles**.

Using the measuring instrument in transmission loss mode reduces the dependence of the measurement on any calibration. Most calibration routines are used to adjust the exact phase response and impedance levels of the measurement. However, the transmission loss measurement is measuring the magnitude of the signal so it is not sensitive to phase. Furthermore, for high Q inductors, the frequencies of measurement are close together so frequency dependent errors are reduced. Similarly, at the amplitude levels where the frequencies are measured differ by only 3 dB, so errors in the log amplitude measurement are also reduced.

Conclusions

A method for measuring the Q of an inductor that is accurate and relatively insensitive to instrument calibration was found. Using a capacitor to form a parallel resonant circuit with the inductor under test provides a circuit where Q can be measured from transmission loss. The measurement circuit was analyzed with *LTspice* to confirm that it was not subject to errors due to the termination loads,

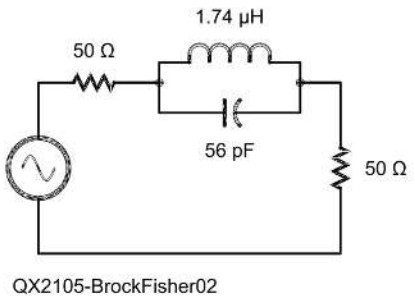

Figure 2 — Parallel resonant Q measurement circuit.

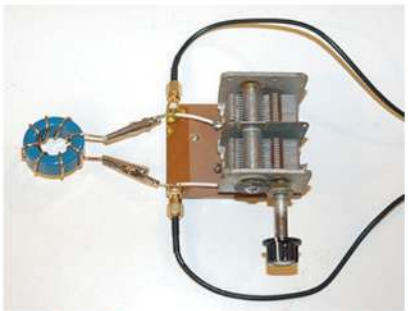

Figure 3 — Parallel resonant circuit fixture for measuring inductor Q.

and to demonstrate that the finite Q of the capacitor did not degrade the measurement significantly. A measurement fixture was described that facilitates connecting an inductor to be measured into the parallel resonant configuration in a transmission loss measurement using a VNA or SA. The computation of Q from three points of the transmission loss versus frequency curve is described. The measured Q of the circuit is a reasonable approximation of the Q of the inductor, as long as the Q of the capacitor is much higher than that of the inductor.

First licensed in 1967 at age 13 as WN1IKP, Tony Brock-Fisher upgraded to Amateur Extra class, changing his call sign to K1KP, in 1976. After getting his BS in Physics and MS in Ocean Engineering he enjoyed a 35 year career as an electronics engineer designing cardiac ultrasound systems for HP, Agilent, and Philips. A past president of Yankee Clipper Contest Club, Tony enjoys contesting, DX, and station construction projects, as well as writing for QEX!

References

[1] R. B. Broberg, NanoVNASaver; **https://nanovna.com/?page_id=90**.

[2] P. Salas, AD5X, "Fixture for Measuring Inductor Q with your Antenna Analyzer;" **www.ad5x.com/images/Articles/QmeterRevA.pdf**.

[3] A. Payne, G3RBJ; **g3rbj.co.uk/wp-content/uploads/2017/12/Measurements-of-Loss-in-Variable-Capacitors-issue-3.pdf**.

[4] G. Murphy, VE3ERP, "The Elusive Q of Single-Layer Air Core Coils," *CQ Magazine*, May 1999.

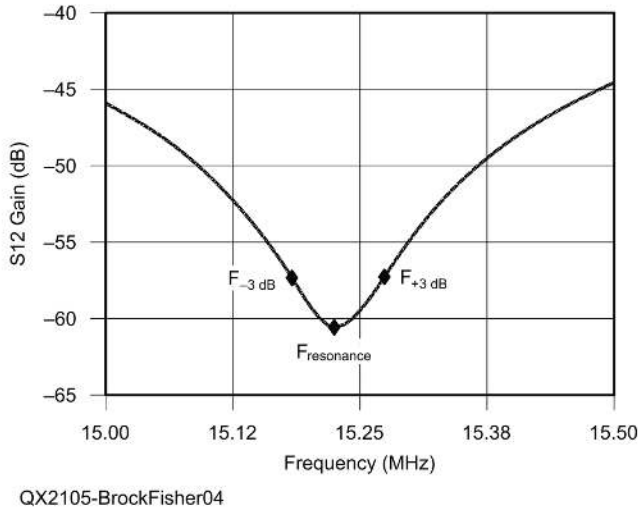

Figure 4 — Transmission loss plot shows the upper 3 dB, resonant, and lower 3 dB frequencies.

Upcoming Conferences

Digital Communications Conference (DCC)

September 17 – 19, 2021

Virtual

https://tapr.org/digital-communications-conference-dcc/

The 40th annual ARRL and TAPR Digital Communications Conference (DCC) will take place, September 17 – 19, 2021. Due to the coronavirus pandemic, this year's conference will be held online.

Technical papers are being solicited for presentation. Papers will also be published in the *Conference Proceedings*. Authors do not need to participate in the conference to have their papers included in the *Proceedings*. The submission deadline is **August 15, 2021**. Submit papers via email to Maty Weinberg, KB1EIB, **maty@arrl.org**. Papers will be published exactly as submitted, and authors will retain all rights.

Paper and presentation topic areas include, but are not limited to, software defined radio (SDR), digital voice, digital satellite communication, digital signal processing (DSP), HF digital modes, adapting IEEE 802.11 systems for amateur radio, Global Positioning System (GPS), Automatic Position Reporting System (APRS), Linux in amateur radio, AX.25 updates, Internet operability with Amateur Radio networks, TCP/IP networking over amateur radio, mesh and peer-to-peer wireless networking, emergency and homeland defense backup digital communications in amateur radio.

John Stanley, K4ERO

524 White Pine Lane, Rising Fawn, GA 30738; **jnrstanley@gmail.com**

A Simple Way to Tune Out SWR on a Balanced Transmission Line at VHF and UHF

Match twin lead or ladder line feeders with a sleeve implementation of a Series-Section Transformer.

Twin lead or ladder line feeders can be matched by using a Series-Section Transformer without cutting the main line. This highly adjustable match uses a foil sleeve that slides along the twin lead. The method is very practical for VHF and UHF applications. It could be used at HF, but the length of the sleeve becomes quite long.

The Series-Section Transformer is well discussed in Section 24.4 of the *ARRL Antenna Book*. This matching method is very useful but has not been applied as often as it might have been because it requires cutting the main line to insert a section with a different Z_0, and because it is not easy to adjust for a perfect match. Formulas are available for determining the location, length and Z_0 of the inserted line and are an easy way to design such a match. Actually, the well known and used quarter wave section at the matching point is a sub-set of this method, as is the twelfth-wavelength transformer. This method was also described in the July, 1978 *QST*. It would be well worth a look at the material in either the *QST* article or the *Antenna Book* for a better understanding of this method.

The use of the *QST/Antenna Book* formulas for design of these lines is perfectly workable. However for those who are familiar with a Smith chart, I think it is more intuitive and faster to simply look for the solution using Smith chart software. That is the method I have used in my study of this subject. We will begin by looking at some examples and finding a Series-Section matching solution.

Consider the case of a 300 Ω line that is matched at the antenna. At the transmitter we wish to feed it through a 50 to 200 Ω balun. This balun would consist of a half wave section of coax connected as shown in **Figure 1**. A 300 Ω load on the 200 Ω balun output would present a 1.5:1 SWR to the transmitter. While that is possibly acceptable, it could cause the transmitter power to begin backing off. Getting the SWR lower is very simple.

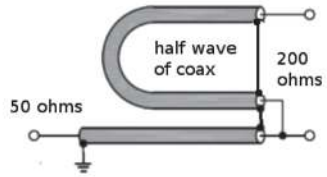

Figure 1 — A 50 to 200 Ω balun.

With a Smith chart **[1]** we can design a match at 144 MHz between 300 and 200 Ω (**Figure 2**). At the 300 Ω point a 2 inch section of 100 Ω line is inserted. This is followed by an 8 inch section of 300 Ω line. However, one may ask, "Isn't it a lot of trouble to cut the 300 Ω line and insert the 2 inch section of 100 Ω line, and in any case where do I get 100 Ω balanced line?" A foil sleeve provides a very simple solution. If we wrap the twin lead or ladder line with a strip of aluminum foil, it will reduce the Z_0 of that section by a large amount, typically down to about 100 Ω. Further discussion of how the foil affects the Z_0 of the line can be found in **Appendix 1**, and power limitations are discussed in **Appendix 2**. So we cut a piece of aluminum foil to about 2 by 2 inches, and wrap it on the twin lead. We place it about

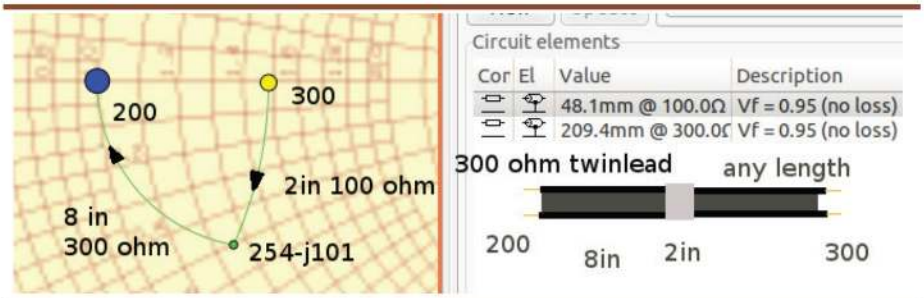

Figure 2 — A 300 to 200 Ω match. The Smith chart is centered on 200 Ω. *LinSmith* was used for these plots.

8 inches from the 200 Ω balun connection. But here is the really nice part. We can slide the aluminum foil up and down the twin lead until we get the lowest SWR at the 50 Ω point. If it is not perfect we can easily shorten or lengthen the 100 Ω section of foil. With a few quick adjustments of length and position of the aluminum foil we can get a perfect match.

Here is another example of the same method. Suppose that we have a low loss 300 Ω line feeding an antenna with an SWR of about 2:1. This means that the complex impedance near the transmitter end will fall at each point on the 2:1 SWR circle at some place along the line. A 79 mm (3.1 inch) sleeve should be installed where the Z is 193 + j 132 Ω, see **Figure 3**.

Slide it up and down the line to find the best match and if needed, change the length of the foil section. Putting the sleeve in the wrong place on the 2:1 circle will increase the mismatch. The location of the matching sleeve is important, but easily found.

This match could have been done at a 193 + j 132 Ω point near the transmitter end of the line, rather than at the antenna end. Matching at the antenna has two advantages: 1) the line loss will be less as there is no SWR on the line; 2) the bandwidth of the match will be broader. The disadvantage of doing it at the antenna might include: 1) the matching has to be done up in the air, where it might be hard to reach; 2) the SWR measuring instrument will be at the transmitter, and thus two people might be required to do the adjustment, one to make the changes and another to read the SWR.

If done at the transmitter end, the same technique would be used. Slide the foil sleeve — which would still be close to the same size as when matching at the antenna — up and down until you find the place where the match is best. If done at the transmitter end we get a narrower band match. However, most of our VHF bands are narrow as a percentage of frequency. If the results are too narrow, put the match closer to the antenna. Outdoor matching sleeves should be well protected from weather, perhaps by using self amalgamating rubber tape, as is commonly done with coax connectors that are exposed. Even if indoors, the sleeve should be protected and kept in place with tape.

The approximate width of the aluminum foil sleeve will be related to the amount of SWR reduction required. As we have seen in the above examples, for 144 MHz, about 2 inches (**Figure 2**) will reduce an SWR of 1.5:1, and a 3.1 inch sleeve (**Figures 3**) will

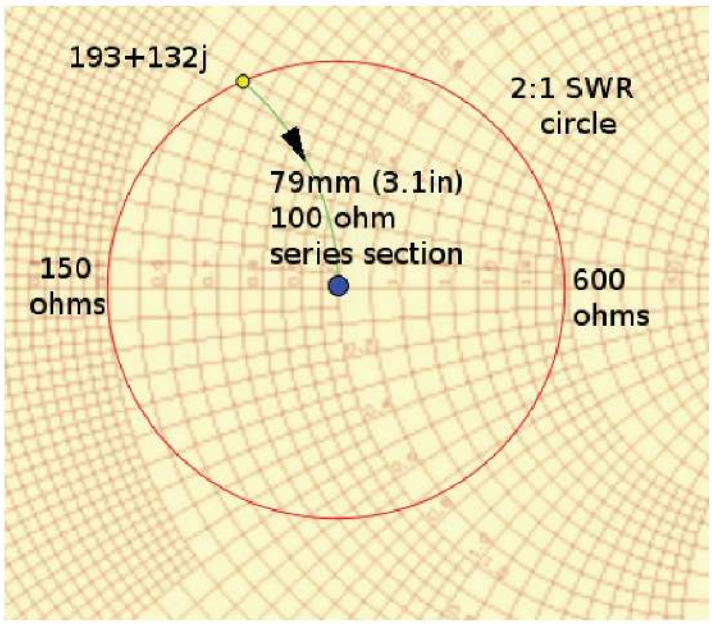

Figure 3 — The circle is the locus of all possible 2:1 SWR values for Z. If a 100 Ω section is inserted where the Z is 193+132j it will pull the Z to 300 Ω for a 1:1 match. Sliding the sleeve along the coax moves it around the 2:1 SWR circle.

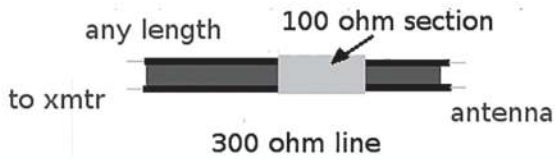

Figure 4 — A 3.1 inch sleeve is wrapped on the 300 Ω line and moved to find the best match.

tune out an SWR of 2:1. For other bands, the length of the basic sleeve (**Figure 4**) will be proportional to the wavelength. Below 6 meters the sleeve may be impractically long. There is no problem with using several sleeves either overlapping or separated by some distance. Overlapping is an easy way to change the total length of the sleeve. There are no longitudinal currents in the sleeve along the twin lead, although there are currents in the circular direction around the wires. For that reason, several turns of foil should be used to provide a good path for those circular currents.

I did some 'real world' tests on JCS #1018 18AWG twin lead. Listed as 300 Ω, Peter Schuch, WB2UAQ, tested it and found it closer to 230 Ω **[2]**. My measurement showed 233 Ω, which is probably the same within the margin of error. This impedance can be lowered to 100 Ω in actual tests, by wrapping it in foil.

I used a short piece of twin lead that measured 1/8 wavelength at 63 MHz to determine the line impedance. The exact length is not important and the electrical length is easily measured by seeing which frequency rotates 1/4 of the way around a Smith chart. I used the formula

$$Z_0 = \sqrt{Z_{short} Z_{open}}\ .$$

The real part of Z will be small so we can simply use the reactance $X_{C\,open}$ and $X_{L\,short}$. Then Z_0 is equal to the geometric mean of the reactance of a 1/8 wave shorted line and the reactance of a 1/8 wave open line, using absolute (positive) value for both reactances. This method is described in **hamwaves.com/zc.measuring/en/index.html**.

If done with complex values for the Z_{open} and Z_{short} lines, the sign of the values should be retained. Complex value for Z_0 can be calculated if the real parts of the measured complex Z values are sufficiently accurate. Since R values are very small they are difficult to measure, but it may be worth a try. Complex values for Z_0 can be used in programs such as *TLW* to give more accurate calculations. However, for most practical RF transmission lines the imaginary part of Z_0 values can be ignored and results will be sufficiently accurate.

Since my nanoVNA in the Smith

chart display reads R plus capacitance or inductance values, I converted them to reactance using standard formulas, or an online calculator **[3]**. Later software versions of the nanoVNA and most lab VNA instruments read R and X directly. For taking the square root of a product of two complex numbers I used an online calculator **[4]**.

A finite element analysis of a reasonable approximation of this line also shows less than 100 Ω to be possible **[5]**.

Figure 5 shows a test of the foil sleeve method described above. A 50 to 200 Ω balun is used at the nanoVNA. A 150 Ω resistive load is on the left end of the twin lead. Without the foil sleeve, the SWR at the 50 Ω point (VNA) was 1.7:1. The sleeve took the SWR down to 1.01:1, essentially a perfect match. The sleeve was slid along the twin lead until the best match was found.

Using the same test setup with 150 Ω on the left end of the twin lead, a match was found at 432 MHz using two smaller sleeves (**Figure 6**). The 50 to 200 Ω balun was operating on its 3rd harmonic. A solution with a single sleeve should be possible, but I quickly found this one using the two small sleeves. By chance, one sleeve affected both the real and imaginary parts of the Z_0 at the 50 Ω point and the other mainly adjusted only the reactive part (center frequency). This made the tuning very easy. The SWR and Smith plots were very similar to those taken on 2 meters. The SWR could be reduced to 1.01 or 1.00 with ease. However, without tape securing the sleeves, they were easily bumped off the optimum point with the SWR rising to 1.05 or so, indicating a need to secure the sleeves with tape.

Application to a Practical Antenna

I have a two-meter band commercially made antenna that has a **T** match (**Figure 7**), which is connected through a built in balun to feed 50 Ω coax. The loss in the rather long main coax was a concern. So I disconnected the balun at the antenna and connected twin lead directly to the **T** match, which is inherently balanced. At the transmitter end, I used a 200 to 50 Ω balun. This left me with an SWR at the 50 Ω point that varied rapidly with frequency between about 1.3:1 and 2:1. As luck would have it, it was 2:1 at 144.2 MHz, the desired operating frequency. I could have shortened the twin lead by a foot or so to move me to one of the 1.3:1 match points, but it was easier to simply use the foil sleeve method to get a perfect match. I didn't have to shorten the twin lead, which was barely long enough already. Furthermore, if I need to operate on a different frequency, I can simply shift the foil sleeve as needed. However, all of the frequencies used in weak signal work were well within a very low SWR range.

I could go back and put the sleeve at the antenna end, but that would require a lot of running back and forth or else help from someone to read off the SWR values at the transmitter end and report to me at the antenna end. I will probably do that sometime, but for now, operating at 144.2 MHz plus or minus a few hundred kHz, matching at the transmitter end is fine. A 1.5:1 SWR on the twin lead line causes little loss. My estimations show that this arrangement has about 1 dB less total feed line loss than with the coax previously used. It was a worthwhile change.

For another practical test, I found a dipole in my junk box that was somewhat longer than a half wave on 2 meters and fed with 20 feet of twin lead. Neither dimension was chosen for any particular frequency, so this approximated a 'random' antenna. Connecting to the VNA through a 200 to 50 Ω balun, I began to wrap randomly chosen foil strips on the twin lead and slide them around. With about 5 minutes of 'fiddling' I found a prefect match. I used two sleeves about 2 inches and 1 inch long near the antenna, and did a final tweak with a 1/2 inch sleeve near the VNA. I am not saying that you will always find a solution without doing a complex impedance measurement at the antenna and using Smith chart analysis to see where to try the matching sleeves, but at least in this case I easily found the match by simply trying different lengths and locations

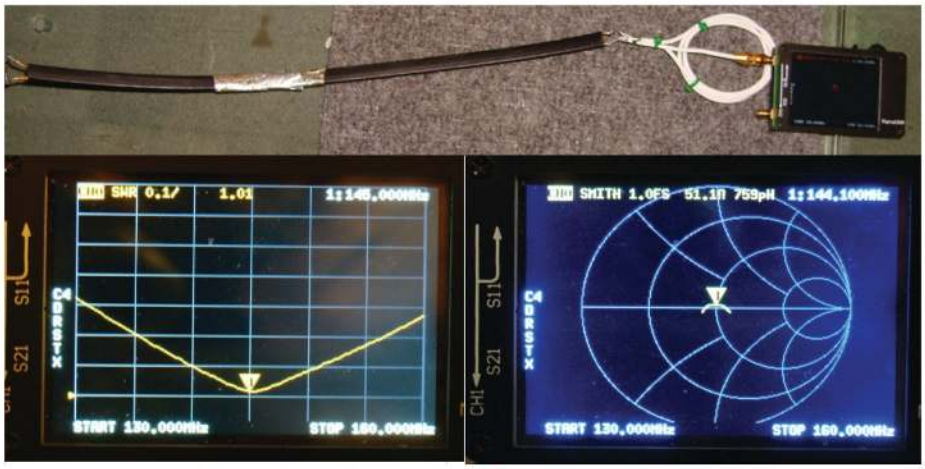

Figure 5 — 150 Ω load matched to 50 Ω on 2 meters.

Figure 6 — 150 Ω load matched to 50 Ω on 432 MHz.

Figure 7 — T match connection to twin lead on 2-meter antenna.

of the sleeve. Since the major part of the match was done near the antenna, I believe that the SWR on the twin lead over the major part of its length was less than 1.3:1.

This opens the possibility of taking whatever antenna you have, say a typical TV antenna or even a pair of 'rabbit ears' and getting it to match on your band of choice. Of course, your balun will have to be suitable for that frequency. I tried to match on 220 MHz using a 144 MHz half wave balun as described above and couldn't find a match even though the balun worked on both 144 and 432 MHz. A broad band ferrite core balun would probably allow almost any antenna to match any band. A larger TV antenna could also be matched and it might have some gain in a useful direction. It is easy enough to give it a try, if you have a twin lead fed TV antenna left over from the days before cable TV **[6]**.

Appendix 1 – How the Foil Sleeve Changes the Z_0 of a Parallel Wire Line

The Z_0 of a lossless transmission line is given by:

$$Z_0 = \sqrt{L/C}$$

where L is the inductance per unit length, and the C is the capacitance per unit length. These can be measured by shorting the end and measuring the L at low frequencies, and by measuring the C of the line with the end open. The length of the measured line is not important as long as it is a small fraction of the wavelength at the measurement frequency, since it is only the ratio of the two numbers that matters.

The formula tells us that if C is increased, the Z_0 will go down. Wrapping a foil sleeve around the insulation that joins the two conductors provides additional capacitance since each wire will 'see' the sleeve. The closer the sleeve is to the wires the greater the additional capacitance. The L is also affected as H fields are limited.

Figure 8 (top) shows a finite element simulation of the magnetic and electrical fields along the line without the sleeve. The H (magnetic) fields encircle the wires, and the E (electric) field lines connect one wire to the other. When a metal sleeve is added, the L value is decreased since the magnetic fields will be restricted to the inside of the sleeve. This effect is similar to what happens when an inductor is enclosed in a can such as was done with IF transformers. This effect is shown in **Figure 8 (middle)**. With the shield the E field lines are much shorter and connect mainly between the wires and the sleeve. This is shown in **Figure 8 (bottom)**. These shorter E field lines mean higher capacitance.

Since C goes up and L goes down, the net result is a reduction in the Z_0 of the line. In the lines I checked, tightly wrapping the sleeve with aluminum foil lowers the Z_0 to about 100 Ω. This is consistent with simulations I made using finite element analysis software. If less effect were desired, one could use a dielectric spacer between the foil and the line. For non-adjustable effects, one could apply copper tape to only one side of the twin lead. Such tape with adhesive is available from stained glass suppliers. Sticky aluminum tape is also sold in hardware stores for sealing HVAC ducts. One could even slip a piece of aluminum tubing over the twin lead. This would be adjustable, but would not lower the Z_0 as much as other options. It might serve for a section that was to pass through a wall.

Appendix 2 – Power Limit Considerations

There may be some concern as to power limits being made lower by the application of the foil sleeve to a balanced line. The voltage rating of the line will certainly be lower as the total space between conductors is reduced. Since the sleeve is applied at a point near the matching circle, both the voltage and current at that point will be no worse than the peak voltage and peak currents on a matched line with the sleeve. Thus SWR on the line does not add to the peak voltage or current limits *at the sleeve*. Operating with high SWR on any transmission line must of course consider the fact that voltage and current will be high at the minimum and maximum reflection points along the coax and this reduces the power rating — peak power rating at the voltage peaks and average power rating at the current peaks.

My tests on the twin lead type JCS #1018 18AWG show no arcing at the sleeve with up to at least 1200 V rms (60 Hz ac), which is equal to 4.8 kW on a 300 Ω line. At 1500 W, a 300 Ω line would carry 2.24 A. The 100 Ω section pulls the line Z to 300 Ω, never lower. Other types of twin lead would need to be tested, especially very thinly insulated TV type ribbon line — probably not a good choice for high power. If needed, Teflon plumber's tape could be wound on under the sleeve or other means used to increase the voltage rating. This would of course place some limit on how low the Z_0 of the matching section could go, meaning it might have to be made longer.

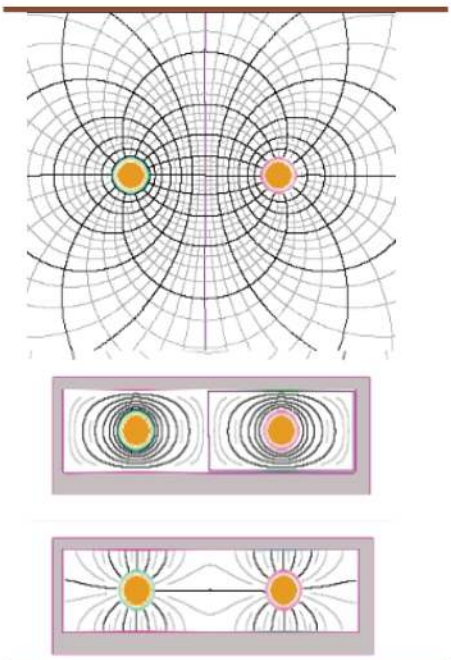

Figure 8 — The top plot shows the twin lead seen end on. The E and H fields fill all of space out to some distance. In the middle and bottom cases, the two wires are enclosed in a metal sleeve. This confines the H fields as shown in the middle plot. In the bottom E field plot, the sleeve allows the E fields to go mainly to the shield instead of to the other wire. More RF current will flow meaning the capacitive reactance is reduced, and the C is increased.

John Stanley, K4ERO, and his wife Ruth, WB4LUA, retired to Rising Fawn, Georgia after 45 years in international broadcasting, where they did engineering, consulting, and training with Christian radio stations in many countries. As an ARRL Technical Adviser for the past 30 years, John has contributed to many ARRL publications.

Notes

[1] Smith chart analysis was done using *Linsmith*: **jcoppens.com/soft/linsmith/index.en.php**.

[2] **https://forums.qrz.com/index.php?threads/jsc-wire-and-cable-twin-lead-data.580208/**.

[3] You can convert capacitance and inductance to reactances using standard formulas, or use this handy calculator: **www.electronics2000.co.uk/calc/reactance-calculator.php**.

[4] *Math Is Fun, Complex Number Calculator*, **www.mathsisfun.com/numbers/complex-number-calculator.html**.

[5] Finite element analysis was done using ATLC2, see: **www.hdtvprimer.com/KQ6QV/atlc2.html.**

[6] For modifying a typical LPDA TV antenna for ham band use, see the article by John Stanley, K4ERO, that comes with the *ARRL Antenna Book CD* as a supplementary file.

Dan Koellen, AI6XG

5098 Foothills Blvd. #3-262, Roseville CA 95747; **ai6xg@arrl.net**

Telegram Your Commands

Remotely command and monitor your ham station from anywhere that you have internet access.

My station, AI6XG, operates its transceiver and antenna remotely. The transceiver, a Flex 6400, is located in an adjacent lot near the station antennas. Being remote, I want to be able to monitor the status of the station and power the transceiver **ON** and **OFF**. Since I can operate from anywhere I have an internet connection, I wanted system control and monitoring available anywhere I have internet access as well.

In this article I describe how to set up your own remote command and monitoring system so you can build a system to meet your needs and configuration.

Why *Telegram*?

I looked at various applications and other solutions for remote monitoring and control. I chose *Telegram*, a cloud based messaging app. With the *Telegram* app you can send and receive messages and commands. *Telegram* has apps for iPhone, Android and Windows phones, and iPad tablet as well as desktop apps for PC/Mac/Linux, MacOS and web browsers. *Telegram* is very versatile, allowing its use from many different operating systems.

Modules for Arduino and Raspberry Pi have been written using the *Telegram Bot* API (**https://core.telegram.org/bots**). A *Telegram Bot* can be built that will respond to messages and commands sent to it. The *Telegram Bot* can also send *Telegram* messages from the system it is installed on to a *Telegram* app.

This means that from your *Telegram* app on your mobile phone, tablet or desktop you can send and receive messages to and from a *Telegram Bot* that is installed on an Arduino or Raspberry Pi. I used a *Telegram Bot* on a Raspberry Pi to implement a monitoring and control system for my remote station. I will show you how to design one for your station.

Set up the *Telegram* app and Get Your *Bot* Access Token

To take advantage of *Telegram* you must first install the *Telegram* app (**Figure 1**) on your mobile phone by downloading the app from Google Play or Apple App Store. Your *Telegram* account is tied to your mobile phone number so it will follow you with any phone change.

Once you have the app installed and your account set up, you are ready to build a *bot* to be used in your application. To do this you will name the *bot* and receive an access token that will be used in your program. The access token is quite long and looks something like this:

123456789:ABCdefGhIJKlmNoPQRsTUVwxyZ

You may want to do the next steps on your computer so the access code is easily copied and inserted into your program. Simply download the *Telegram* app from the *Telegram* website (**https://telegram.org**); for your operating system and sign in.

Figure 1 — *Telegram* logo.

To create a new *bot*, search for 'BotFather' in the *Telegram* app to bring up BotFather (**Figure 2**).

BotFather is a *bot* itself and will assist you in generating a new *bot*. Type in '/start' to start BotFather, notice that commands in

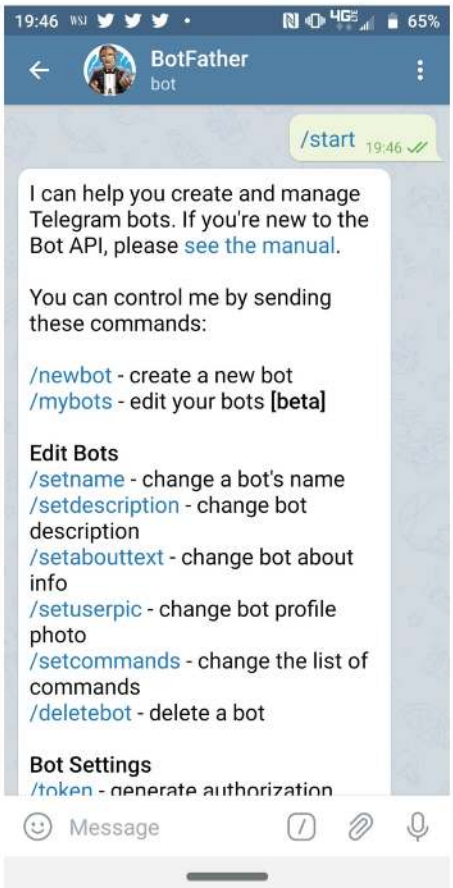

Figure 2 — Start building a new bot with BotFather and the '/start' command.

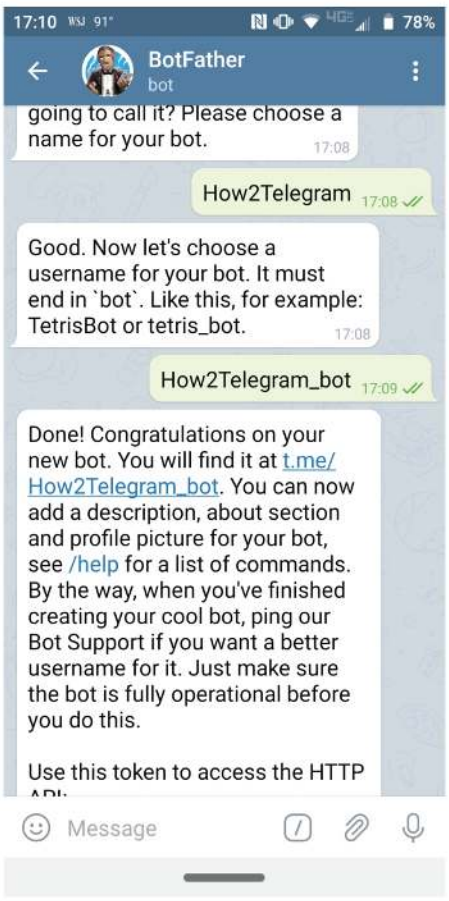

Figure 3 — After entering the '/newbot' command, enter the Bot name (How2Telegram) and username (How2Telegram_bot), and the BotFather will return your access token.

Telegram start with a forward slash (more on this later).

Select /newbot to create your *bot* (**Figure 3**). You will be asked to name your *bot* (e.g. How2Telegram) and provide a username (e.g. How2Telegram_bot) that must end in 'bot'. Once you enter the username the access token is generated. Copy it for later use.

Setting up the *Bot* in Python 3

We will be using *python-telegram-bot* python package to use the *Telegram bot* on a Raspberry Pi. The GitHub page (**https://github.com/python-telegram-bot/python-telegram-bot**): for *python-telegram-bot* has extensive documentation, references and examples.

First, we must install *python-telegram-bot* on the Raspberry Pi by using the following from the command line:

sudo apt-get install python3-pip

sudo pip3 install python-telegram-bot --upgrade

This will install *python-telegram-bot* for Python 3 on your Raspberry Pi. Now let's use a short script that will build your *Telegram bot*. Use the Python IDE in the Raspberry Pi desktop and try the script *test_account.py*. Scripts are at: **https://github.com/phase2682/HowToTelegram** and **www.arrl.org/QEXfiles**.

In *test_account.py* we will use *Telegram* API to confirm that your *bot* is functional. After we import *Telegram* the *bot* is built by

hambot = telegram.Bot(token)

where token is the access token generated earlier. The function *hambot.getMe( )* returns basic information about the *bot*. The information that is printed out should match the information you supplied when you made the new *bot*. It can take a minute or two before the information is returned by the function.

Listening and Replying

For monitoring and control we want the *Telegram bot* to listen for any messages or commands sent to it. We want the *bot* to wait for a message or command, act on it and then wait for more messages and commands. To do this, we use the *python-telegram-bot* to link to the *bot* and handle any messages or commands sent to the *bot*. The class *updater* is used to establish the link to the *bot*; we will setup *updater* as a polling service. When messages or commands are received by the *bot*, *dispatcher* (part of *updater* class) will send them to the appropriate handler. The *handler* will act by taking an action you define. These classes and modules must be imported by using:

from telegram.ext import
Updater, CommandHandler,
MessageHandler, Filters

In the script *listen_for_message.py*, we set up *hambot* as the *Telegram bot* and a message handler to respond to a dispatched message by directing to the function *action(msg)*. See **Code Snippet – 1.**

Here the *bot* replies with the message sent to it and the sender's id; this is defined in the *action* function. Take note of your sender id, we will use that later. In this message handler we use the very handy *Filters* module, which has several predefined filters. In this example the message handler will react to messages *(Filters.text)* but not to commands *(~Filters.command)*.

Now that we have the *bot* listening and replying to messages, we can make the *bot* take actions depending on the content of the message. The script *reply_to_message.py*, *action(msg)* will test for specific words or phrases contained in the message. For example, the **Code Snippet – 2** will return the current date if either 'date' or 'Date' is received in the message.

You can also set up the action for specific commands that in *Telegram* are preceded by a forward slash. We do that with the *'/time'* command by using a handler for commands only; see **Code Snippet – 3**, which will return the current time if only *'/time'* is sent. The text can not contain any other content. The *handler* class has other specific handlers; we will use only command and message handlers in this article but take a look at the other handlers that can be used.

The function *context.bot.send_message(chat_id, text)* sends a message to the *Telegram* user with the id 'chat_id'; 'text' is the string content of the sent message. If you are responding to the user that sent the original message you can use the simpler *update.message.reply_text (text)*.

My experience working with *dispatcher* has been that *handlers* are called in order. This script uses that to respond to unknown commands by the very last handler to react to commands not handled by preceding handlers.

Try different combinations of words and capitalization to see how the *bot* responds.

Make the *Bot* do Something

We are going to set up a simple circuit to show that the *Telegram bot* will respond to a message by changing an output. This can be used to turn **ON** equipment, or to **SWITCH** antennas. For example, the Flex 6400 will power up or shut down according to a logic state applied to a back panel input.

We will also monitor the status of the circuit and respond with a message indicating the status. At my station, AI6XG, +5 V from the Flex 6400 USB port is monitored to determine whether the transceiver is powered up or not.

In this example an LED will be turned **ON** and **OFF** by the *Telegram bot*. When the LED changes state, *Telegram* sends a message with the LED status.

We will be using the script *do_something.py* to demonstrate changing an output and monitoring for changes. As shown in **Figure 4** we are using the Raspberry Pi to turn the LED **ON** or **OFF** (GPIO 21) while the Raspberry Pi is also monitoring the status of the LED (GPIO 20). Normally we would not use one pin to monitor another pin but this is just a demonstration circuit.

To turn the LED **ON** or **OFF**, the *bot* will change GPIO 21 state according to the incoming message or command and

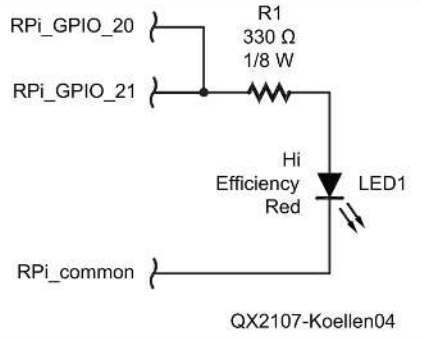

Figure 4 — Circuit for bot demonstration.

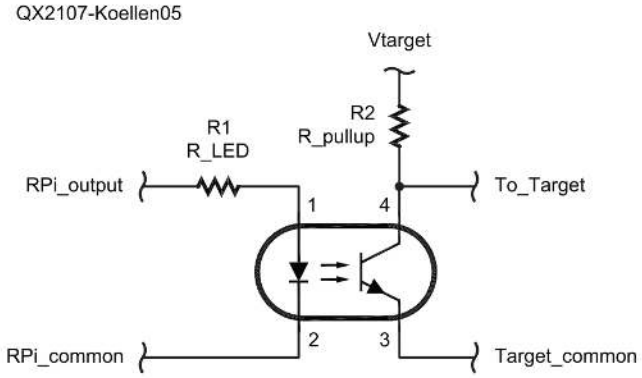

Figure 5 — Isolating a RPi output. R1 limits the current to the opto-isolator internal LED; for the Raspberry Pi 3.3 V output a 180 to 200 Ω 1/8 W resistor can be used for 10 mA of LED forward current. For a typical 5 V input, R2 can be 10 kΩ to 100 kΩ 1/8 W.

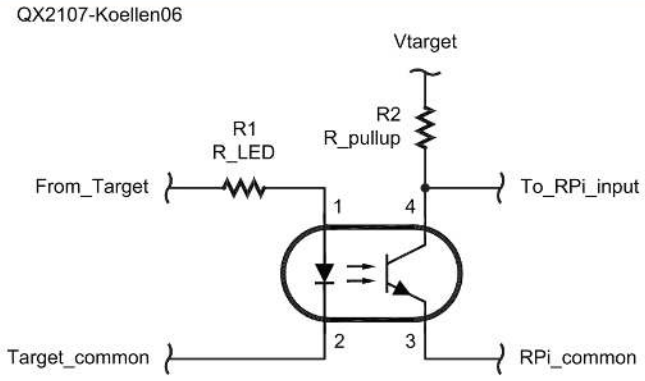

Figure 6 — Isolating a RPi input. R1 limits the current to the opto-isolator internal LED; for 5 V targets a 330 Ω 1/8 watt resistor typically is used for 10 mA of LED forward current. For a 3.3 V input, R2 can be 10 kΩ to 100 kΩ 1/8 W, or the internal pull up on a Raspberry Pi can be used.

send a confirming message that the LED is changing state. In this script both message and command handlers are used to turn the LED **ON** or **OFF**, or report its status. In an actual application two types of handlers would not be used for the same response. In this example though, we are demonstrating two different ways of implementing *bots* to take action. Also, only one output is used in this example, while the Raspberry Pi has several more GPIOs that can be used in a similar fashion.

We use an interrupt on the input that is monitoring the LED to detect a change of LED state and then send a status message (**Code Snippet – 4**). This is executed by the function *on_off(pin)* that is pointed to by the interrupt (**Code Snippet – 5**).

Since the *bot* is running in a different thread we can not send a message using the *bot* during an interrupt. Instead the message is sent using the *Telegram* API (**Code Snippet – 6**).

For this demonstration script we added a test for authorized users before reacting to a message. First a list of authorized users is built, 'you' is your user id from running *listen_for_message.py script*. You can also use the 'get id' *bot* in your *Telegram* app to return your user id, (**Code Snippet – 7**).

By using *Filters* it is very easy to specify that a handler acts only on messages or commands from authorized users:

LedOn_handler =
CommandHandler('LedOn',
LedOn, Filters.chat(users))

The application here is a simple example of what can be done with a *Telegram bot*. We can do more than just turn **ON** an LED; the Raspberry Pi outputs can be used to turn **ON** or **OFF** equipment, change antennas through a digital antenna switch, turn **ON** indicators, etc.

Likewise, monitoring can be done with many other applications. At my station, AI6XG, the temperature and humidity of the outdoor enclosures is monitored in addition to the status of the transceiver. A simple message to the *Telegram bot* returns a temperature and humidity report. I use this monitoring to determine if the transceiver needs to be shutdown during some of our extreme summer heat to prevent overheating. Conversely, the monitor instructs me to keep the transceiver idling to maintain the vented enclosure humidity at a safe level during winter rains.

A Few Notes on Interfacing to the Raspberry Pi

The Raspberry Pi is a very useful single board computer but one has to be careful when using its inputs and outputs. The inputs and outputs are not 5 V tolerant; no more than 3.3 V should be applied to an input. Likewise, an output driven high will deliver only 3.3 V with limited current.

For the installation at AI6XG all inputs and outputs going to external equipment were connected through an opto-isolator. The opto-isolator has a few important roles. It isolates the Raspberry Pi from the transmitting and receiving equipment that could be operating at higher voltages than the Raspberry Pi can tolerate. It also acts to isolate the common returns (ground) of the Raspberry Pi from the transmitting and receiving equipment. The opto-isolator can be used to convert the 3.3 V output to another voltage (like 5 V) or protect the Raspberry Pi inputs from signals greater than 3.3 V.

In **Figure 5** the opto-isolator is isolating the Raspberry Pi output from the target equipment. The pull up resistor on the output of the opto-isolator can be used to shift the voltage required by the target equipment, often 5 V.

Likewise, in **Figure 6**, the input of the Raspberry Pi is isolated from the monitored target. An external pull up resistor can be

used on the opto-isolator output to pull to 3.3 V or an internal pull up can be used.

The resistor on the input of the opto-isolator is the current limiter for the internal LED. I recommend using opto-isolators with LED forward currents that are less than 10 mA for compatibility with the Raspberry Pi GPIO.

The circuit shown in **Figure 7** does not provide any isolation but can be used for voltage translation or provide more current than the Raspberry Pi can provide. A FET can also be used for this circuit.

To switch higher voltages and currents there are a number of components that can

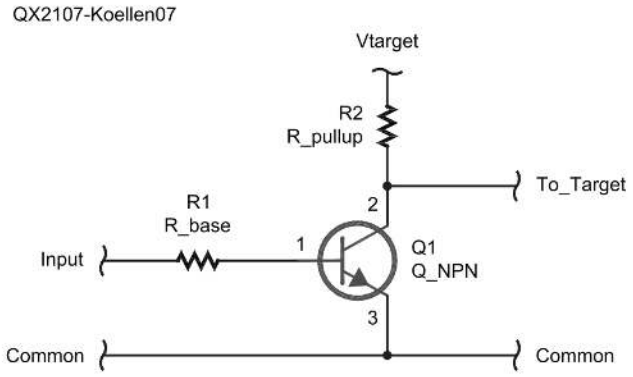

Figure 7 — Non-isolated voltage translation. Q1 is a general purpose NPN transistor. Use R1 to set the appropriate base current, and R2 is a pull up and current limit for the target.

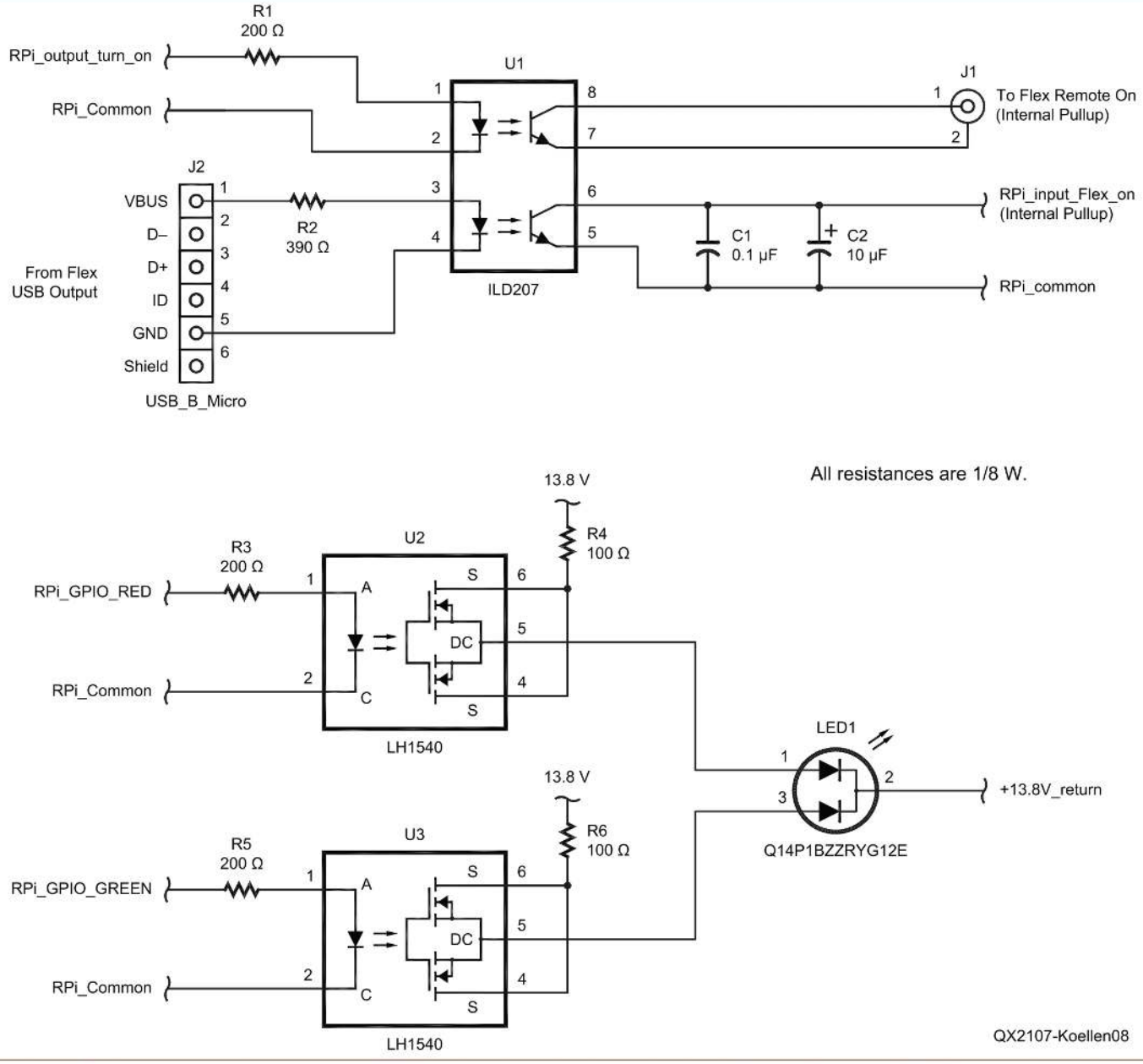

Figure 8 — Schematic of the system used at AI6XG to control and monitor the status of a Flex 6400. U1 is a ILD207 dual opto-isolator. J1 is a phono jack and J2 is a microUSB jack. C1 and C2 are noise reduction capacitors rated 6.3 V or greater. U2 and U3 are LH1540 normally open SSRs, LED1 is an APEM Q14P1BZZRYG12E red and green LED weather proof assembly.

be used with the Raspberry Pi. There are multi-channel solid state relay (SSR) boards available from Amazon and eBay that can switch ac voltages up to 240 V and 2 A. These boards have integral opto-isolation to completely isolate the switched output from the input logic signal. Some of these boards can require 5 V logic signal to switch the SSR, the circuit in **Figure 7** is handy for translating the Raspberry Pi 3.3 V logic to 5 V logic. Remember that the logic signal is inverted when using this circuit.

There are also single channel devices that are an opto-isolated SSR in a small footprint. I have successfully used the LH1540 for low current switching. Also, IXYS has a nice selection of opto-isolated SSRs including the CPC1510 for moderate currents. For higher current and voltage, the OMRON G3MC-202P-DC5 is suitable.

Figure 8 shows an example of different interface configurations, and is a portion of the system used at AI6XG to control and monitor a Flex 6400. An output from the Raspberry Pi is used to drive the 'remote power on' input of the Flex 6400 to power it **ON** and **OFF**. The +5 V from the Flex USB output is used as a power up monitor, driving an input of the Raspberry Pi. In addition, a weather tight dual LED indicator is driven using LH1540 SSRs. When the Flex is powered up the green LED is illuminated, while the red LED is illuminated when the Flex is powered down. The indicator LED is mounted on the enclosure so the status can be casually checked from the outside. Also, the Raspberry Pi tracks how long the system has been **ON** or **OFF** and if the *bot* was successful in executing a command.

Summary

There are many possibilities for monitoring and remote operating using *Telegram* and a Raspberry Pi single board computer. I have shown a few examples of how to implement an internet-connected control and monitoring system that you can connect to anywhere you have internet access. Use these examples to expand and adapt for your setup and have some fun while you are at it!

Dan Koellen, AI6XG, has held an Amateur Extra class license since 2017. He earned his Novice license, WN9JHZ, in 1973 and the Advanced class license, WB9TCU, in1981. Dan has been designing and building electronic projects since his teen years. He holds a BS in applied math, engineering and physics from the University of Wisconsin-Madison, and an MS in engineering and applied science with from Southern Methodist University in Dallas. He is now retired from a profession in the semiconductor industry where he specialized in semiconductor device reliability physics, failure analysis, quality program implementation and supply chain management. Dan's ham radio interests include SOTA activation and chasing, HF CW, and building antennas especially for SOTA. He is also interested in microcontrollers and single board computers, using assembly language, C, C++ and Python. Dan especially enjoys applying technology to his garden.

Code Snippet – 1.

```
updater_hambot = Updater(token)                                    #establishes update link to bot
dispatcher_hambot = updater_hambot.dispatcher                      #dispatches the updates
updater_hambot.start_polling()                                     #starts polling service
                                                                   #to get updates from Telegram


#handler for messages
msg_handler = MessageHandler(Filters.text & (~Filters.command), action)
dispatcher_hambot.add_handler(msg_handler)                         #adds msg handler
```

Code Snippet – 2.

```
elif 'date' in message or 'Date' in message:
        context.bot.send_message(chat_id, str('Date: ') + now.strftime ("%B %d, %Y UTC"))
```

Code Snippet – 3.

```
#handler for /time
time_handler = CommandHandler('time', time)
dispatcher_hambot.add_handler(time_handler)          #adds /time handler
```

Code Snippet – 4.

```
#add interrupt on LED_mon
gpio.add_event_detect(LED_mon, gpio.BOTH, on_off, 100)
```

Code Snippet – 5.

```
#thread that runs on an interrupt
  def on_off(pin):
        if gpio.input(pin):
              turn_on_time = datetime.datetime.utcnow()
              telegram_send_message("LED just turned on" + turn_on_time.strftime(" at %H:%M:%S on %B %d, %Y UTC"),
              token, you)

        if not gpio.input(pin):
              turn_off_time = datetime.datetime.utcnow()
              telegram_send_message("LED just turned off" + turn_off_time.strftime(" at %H:%M:%S on %B %d, %Y UTC"),
              token, you)
```

Code Snippet – 6.

```
  #define send message to telegram
  def telegram_send_message(message_text, bot_token, chat_id):

        send_text = 'https://api.telegram.org/bot' + bot_token + '/sendMessage?chat_id=' +str(chat_id) +
        '&parse_mode=Markdown&text=' + message_text

        response = requests.get(send_text)

        return response.json
```

Code Snippet – 7.

```
#list of authorized users
users = [you, ham2]
```

Get Prepared for POTA, SOTA, YOTA, and More!

Coaxial Cable Assemblies

These low-loss cable assemblies are available in standard lengths with DX Engineering's revolutionary patented PL-259 connectors. Use the online Custom Cable Builder at DXEngineering.com to build assemblies made to your exact specs. DX Engineering's coaxial cable is also available by the foot or in bulk spools. **Enter "Coaxial Cable Assemblies" at DXEngineering.com.**

PicoAPRS and PicoAPRS-Lite

WiMo

Developed for balloon tracking, the versatile PicoAPRS-Lite Transceiver Module features automatic or manual frequency tuning, integrated GPS module with balloon mode, and temperature/air pressure sensor. It easily fits in your pocket or installs out-of-sight in your vehicle. Version 3 of the matchbox-size, fully configured PicoAPRS Transceiver with GPS Receiver has an APRS tracker, a receiver for APRS data, Terminal Node Controller, up to 1W of transmit power, and loads more. **Enter "WIMO APRS" at DXEngineering.com.**

bhi · HEIL SOUND · INRAD international radio

Headsets and Headphones

DX Engineering carries a great selection of hands-free headsets and state-of-the-art headphones from bhi, Heil, INRAD and other top brands. Don't accept anything less than clear, intelligible speech fidelity whether you're doing the speaking or listening. **Click on "Audio" at DXEngineering.com for the full lineup.**

plasticase NANUK PROFESSIONAL PROTECTIVE CASES · RigExpert®

RigExpert Analyzer and NANUK Case Combos

In the field, an antenna analyzer is especially at risk for weather and shock damage. We've paired select RigExpert Antenna Analyzers with perfectly sized NANUK equipment cases. Each case is filled with cubed, sectioned foam for custom configuration. Available separately or in combos. **Enter "Analyzer Combo" at DXEngineering.com.**

ICO-LC-192

ICO-IC-705

Icom IC-705 HF/50/144/430 Portable Transceiver

ICOM

With the features and functionality of the IC-7300, IC-7610, and IC-9700, Icom's new QRP rig is like owning a base transceiver you can hold in one hand. It boasts SDR Direct Sampling technology for stellar transmit and receive performance; 4.3" color touchscreen; real-time spectrum scope and waterfall display; built-in Bluetooth®; wireless LAN; and full D-STAR capabilities. IC-705 accessories include backpack (ICO-LC-192), compact automatic tuner (ICO-AH-705), and magnetic loop antenna (ICO-AL-705). **Enter "IC-705" at DXEngineering.com.**

SB SOTABEAMS

SOTABeams Masts and Portable Wire Antenna Kits

SOTABeams' lightweight, pre-assembled multi-band dipole antenna kits make it simple to receive and transmit strong signals anywhere you go. Choose from several models, including the 80/40/30/20M Band Hopper, rated at 125W. Also bring along SOTABeams' masts, such as the heavy-duty Tactical 7000hds and MINI Telescopic Fiberglass Pole, for fast deployment and worry-free operating. **Enter "SOTABeams" at DXEngineering.com.**

AlexLoop

AlexLoop HamPack Portable Magnetic Loop Antenna System

PY1AHD, Alexandre Grimberg brings more than five decades of Amateur Radio experience to the new AlexLoop HamPack, the ultimate magnetic loop antenna solution for portable operating. The HamPack comes with the widely acclaimed transceiver QRP 40-10M AlexLoop antenna; reinforced, full-size backpack that accommodates the antenna, accessories, and any size QRP rig; and upgraded, easy-to-use tuner. **Enter "AlexLoop" at DXEngineering.com.**

YAESU · ICOM · KENWOOD · ALINCO · CHAMELEON ANTENNAS · VIBROPLEX · M² · samlexamerica

Request Your New Catalog Today!

DX® ENGINEERING

Ordering (via phone) Country Code: +1
9 am to midnight ET, Monday-Friday
9 am to 5 pm ET, Weekends

Phone or e-mail Tech Support: 330-572-3200
9 am to 7 pm ET, Monday-Friday
9 am to 5 pm ET, Saturday

Ohio Curbside Pickup:
9 am to 8 pm ET, Monday-Saturday
9 am to 7 pm ET, Sunday

Nevada Curbside Pickup:
9 am to 7 pm PT, Monday-Sunday

800-777-0703 | DXEngineering.com

ON ALL BANDS · YouTube

We're All Elmers Here! Ask us at: Elmer@DXEngineering.com
Email Support 24/7/365 at DXEngineering@DXEngineering.com

THE BRAINS OF THE OPERATION

BAR GRAPH
Visual representation of all gain and front-to-rear of all antennas

MAXIMUM GAIN MODE
Optimized for max gain

MAXIMUM FRONT-TO-REAR MODE
Optimized for best front to rear

3/4 MODE
Turns the BigIR vertical into a 3/4 wave antenna on 21-54 MHz

BEAM WIDTH
Lets you know the beam-width of chosen antenna designs

OptimizIR

The OptimizIR electronic controller is available as an upgrade for all SteppIR antenna products or as a standalone purchase.

AUTOTRAK
Antenna follows your radio wherever you tune for an optimized experience on every frequency

CUSTOM ANTENNA MODELS
Upload your models to controller

BI-DIRECTIONAL MODE
Simultaneous gain in opposite directions

180 MODE
Reverse directions at the click of a button

ELEMENT RETRACT MODE
Retract element during extreme weather events

steppIR COMMUNICATION SYSTEMS

FOR PRODUCT DETAILS AND ORDERING:
www.steppir.com 425-453-1910